Coordination Chemistry Reviews, 63 (1985) 161–215
Elsevier Science Publishers B.V., Amsterdam – Printed in The Netherlands

COORDINATION CHEMISTRY OF ORGANOMERCURY(II) INVOLVING PHENANTHROLINES, BIPYRIDINES, TERTIARY PHOSPHINES/ARSINES AND SOME RELATED LIGANDS

T.S. LOBANA

Department of Chemistry, Guru Nanak Dev University, Amritsar 143005 (India)

(Received 9 September 1983; in revised form 1 June 1984)

CONTENTS

A. INTRODUCTION

The coordination chemistry of organomercury(II) is not as extensive as that of mercury(II) salts such as halides or pseudohalides, probably because organomercury(II) derivatives have less tendency to increase their coordination by interaction with donor molecules. Nevertheless, the interaction of organomercurials, though weak, can be found in biological systems such as amino acids, sulfhydryl groups, phenanthrolines, bipyridines and organophosphorus/arsenic substances such as phosphines/arsines. To quote a few applications, several organomercury quinolin-8-olates have been used as pesticides in seed dressings because of their antifungal and disinfectant

0010-8545/85/$19.25

activity, and for controlling crop diseases. Similarly, the complex of phenylmercury(II) acetate with triethanolamine is used as a bactericide for agricultural purposes [1–5]. Further, it is well-known that organomercury(II) derivatives, particularly methylmercury(II), cause serious damage to the brain and nervous system because of their transportation in blood and binding to sulfhydryl groups of hemoglobin in the red cell [6,7].

In the present review, the literature (up to 1982) dealing with complexes of organomercury(II) with important ligands such as 1,10-phenanthroline, 2,2′-bipyridine and their derivatives, tertiary phosphines/arsines, 8-hydroxyquinolines and related ligands has been compiled and discussed systematically.

TABLE 1

Names and abbreviations of the ligands

Name	Abbreviation
1,10-Phenanthroline	phen
2,9-Dimethyl-1,10-phenanthroline	2-dmp
4,7-Dimethyl-1,10-phenanthroline	4-dmp
5,6-Dimethyl-1,10-phenanthroline	5-dmp
2,4,7,9-Tetramethyl-1,10-phenanthroline	2-tmp
3,4,7,8-Tetramethyl-1,10-phenanthroline	3-tmp
2,2′-Bipyridine	bpy
3,3′-Dimethyl-2,2′-bipyridine	3-dmbpy
4,4′-Dimethyl-2,2′-bipyridine	4-dmbpy
5,5′-Dimethyl-2,2′-bipyridine	5-dmbpy
6,6′-Dimethyl-2,2′-bipyridine	6-dmbpy
1,2-Diaminoethane	en
1,3-Diaminopropane	3-pn
1,4-Diaminobutane	bn
N,N,N′,N′-Tetramethyl-1,2-diaminoethane	tmed
8-Hydroxyquinoline	oxine
2-Methyl-8-hydroxyquinoline	meoxine
1,5-Diaminopentane	5-pn
Triethylenetetramine	tren
o-Phenylenediamine	opd
2,2′,6′,2″-Terpyridyl	terpy
4,4′,4″-Triethyl-2,2′,6′,2″-terpyridyl	Et_3terpy
Bis(2-pyridyl)methanes	py_2CR_2 (R = H, Me, Et)
Tris(2-pyridyl)methane	py_3CH
Trialkyl- or aryl-phosphines	Ph_3P, Me_3P, Et_3P, $PhMe_2P$
Triphenylphosphine oxide	Ph_3PO
Triphenyl- or triethyl-arsines	Ph_3As, Et_3As
Methylenebis(diphenylphosphine/arsine)	mdp/mda
1,2-Dimethylenebis(diphenylphosphine/arsine)	dmdp/dmda
o-Phenylenebis(dimethylarsine)	opda

Among the various techniques used for structure elucidation, X-ray diffraction (single crystal) is the only reliable technique. However, in recent years ^{199}Hg NMR spectroscopy has emerged as a potentially useful tool for structure elucidation of mercury(II) complexes. Table 1 contains abbreviations of the ligands used.

B. PREPARATIONS OF SOME MERCURIALS

A brief description of the methods of preparation of some important organomercurials is presented in this section. For example, diphenylmercury(II) can be conveniently obtained by the Grignard reaction in ether [8].

$$2PhMgBr + HgCl_2 \xrightarrow{N_2\ atm} Ph_2Hg$$

The yield is quite high (85%). The method for the preparation of Ph_2Hg given by Gilman and Brown [9] involves extraction with $CHCl_3$. A number of related diarylmercury(II) compounds have been obtained by reaction of $N_2H_4 \cdot H_2O$ with arylmercury chloride in ethanol [10]. Reactions of arylmercury chloride with copper powder in benzene also lead to the formation of diarylmercury(II) compounds [11]. The preparation of phenylalkynylmercury(II) derivatives ($PhHgC{\equiv}X$) involves the reaction of an acetylenic compound with PhHgX (X = Cl, Br) in THF or liquid ammonia [12].

The irradiation of Ph_2Hg and PhI in benzene in a quartz vessel gives 70% PhHgI and 20% unchanged Ph_2Hg [13]. Arylmercury halides (PhHgCl, etc.) have been prepared by the reaction of HgX_2 with Ph_4Sn in benzene or THF [14].

Fluoroderivatives such as $(C_6F_5)_2Hg$, $(C_6F_5)HgX$ (X = Cl, Br, I), $(CH_3)(C_6F_5)Hg$ and $(Ph)(C_6F_5)Hg$ have been reported by Livingstone et al. [15] and other workers [16,17] (see refs. 18 and 19 for IR spectra of some organomercurials).

C. SURVEY OF THE LITERATURE; STRUCTURAL AND OTHER ASPECTS OF THE ADDUCTS

(i) Adducts of diaryl-, bis(halogenoalkyl- or aryl-)mercury(II)

The known diaryl- or bis(halogenoalkyl- or aryl-)mercury(II) complexes, as well as techniques used for studying them, are given in Table 2. It is apparent from the table that Ph_2Hg and substituted or unsubstituted dialkynylmercury(II) are the only non-halogen diorganomercury(II) substrates

known to form a limited number of complexes. In contrast, the halogen-substituted diorganomercury(II) substrates form a variety of complexes with different ligands. Obviously the former category of organomercurials has lower Lewis acidity than the latter category.

The adducts of phen, 2-dmp and 2-tmp with Ph_2Hg are of composition Ph_2HgL_2 [20,21]. The IR spectra of the adducts (1600–400 cm^{-1}) do not show ligand coordination. However, in the far-IR spectrum (400–70 cm^{-1}) of $Ph_2Hg(2\text{-dmp})_2$, the X-sensitive mode *t* of the PhHg group near 250

TABLE 2

Adducts of diaryl-, bis(halogenoalkyl- or aryl-)mercury(II) substrates

Compound	Ligand (L)	Techniques used [a]	Ref.
1. Ph_2HgL_2	phen, 2-dmp and 2-tmp	IR, UV, mol. wt. and X-ray	20–22
2. $(RC_2)_2HgL$			
(a) R = Me, $ClCH_2$, $BrCH_2$	phen, 2-dmp	IR	23, 24
(b) R = Ph	phen	IR and X-ray	23, 35
3. (a) $[PhHgC_2R]L$ (R = Me, Ph, CH_2Cl)	phen	IR	12
(b) $[PhHgC_2H]L_2$	phen	IR	12
4. (a) $(C_6F_5)_2HgL$	bpy, phen, dmdp, 4-dmbpy, 2-tmp, en, opda	IR, UV, mol.wt. and X-ray	15, 17, 25
(b) $(C_6F_5)_2HgL$	Ph_3P, Ph_3PO, dmda	IR, UV, mol.wt. and X-ray	15, 17, 25
(c) $(C_6F_5)_2HgL_{1/2}$	mdp, mda	X-ray	26
(d) $(C_6F_5)_2HgL$	bpy, phen, en, bn, 3-pn tmed	t.g.a.	27, 28
5. R_2HgL			
(a) R = CF_3, C_2F_5 and C_3F_7	phen, bpy	IR and mol.wt.	29
(b) R_2HgL_n (R = CF_3, $(CF_3)_2CF$, C_2F_5, (CF_3CFH) and CF_3CH)	$n = 1$ for en $n = 2$ for C_4H_8SO	solution phase IR studies	30
(c) R_2HgL_n (R = CF_3, CF_2CFCl, CF_3CF_2, CF_3CH_2 and $(CF_3)_2CF$)	$n = 2$ for Ph_3P $n = 1$ for mdp, dmdp	^{31}P NMR studies	31
(d) $(Cl_2C{=}CCl)_2HgL$	bpy, phen, 2-dmp, 3-tmp and dmdp	IR, ^1H NMR ^{35}Cl NQR and mass studies	32

[a] Unless otherwise stated all systems in this table (and subsequent tables) deal with synthesis and characterization of adducts.

cm^{-1} differs slightly from that of the free mercurial (258s, 252s and 248sh cm^{-1}) and the X-sensitive mode *u* at 207 cm^{-1} in Ph_2Hg is split into two components (216 and 205 cm^{-1}) [33]. Thus, the environment of Ph_2Hg appears to be changed in the adducts. The UV absorption bands of the adducts do not show the expected shifts to longer wavelengths from free ligand values often observed for phenanthroline complexes [34]. Molecular weight studies (in $CHCl_3$ and benzene) indicate their complete dissociation into Ph_2Hg and the ligand. X-ray powder photographs indicate formation of the adducts. Canty and Gatehouse [22] have carried out a single crystal X-ray study for adducts of 2-dmp and 2-tmp. The complex $Ph_2Hg(2\text{-dmp})_2$ has space group $P\bar{1}$ with appropriate *Pm* symmetry while the adduct of 2-tmp has *Cm* space group (Table 3). The planar ligands of the adducts lie in the (040) plane with linear C–Hg–C units of Ph_2Hg moieties aligned in the (010) direction. Each Ph_2Hg moiety has one ligand adjacent to it with Hg–N distances of 2.8–3.0 Å, and one-half of the ligands in the crystals do not have a mercury atom adjacent to their nitrogen atoms. In the unit cell of each adduct, every second (040) plane has 0.5 occupancy for two Ph_2Hg moieties with mercury atoms in those planes, and every other plane has 0.8 and 0.2 occupancy for two Ph_2Hg moieties in those planes, giving one Ph_2Hg for every two ligands (Figs. 1 and 2). Since the accuracy of Hg–N distance determined from difference Fourier synthesis is uncertain, it is not

TABLE 3

X-ray diffraction data of the adducts

Compound	Space group	Other parameters				*Z*	Ref.
		a (Å)	*b* (Å)	*c* (Å)	Angle (deg)		
$Ph_2Hg(2\text{-dmp})_2$	$P\bar{1}$	15.42	14.28	14.55	$\alpha=\beta=\gamma=90$	4	22
$Ph_2Hg(2\text{-tmp})_2$	*Cm*	21.09	14.54	14.65	$\beta=120$	4	22
$(PhC_2)_2Hg(phen)$	$P2_1/n$	22.564	9.577	10.339	$\beta=96.20$	4	35
$(C_6F_5)_2Hg(mda)_{1/2}$	$C2/c$	14.07	17.34	19.33	$\beta=91.3$	4	26
$[MeHg(bpy)](NO_3)$	$P\bar{1}$	10.229	9.289	6.841	$\alpha=88.98$ $\beta=105.57$ $\gamma=84.81$	2	36, 37 89
$[MeHg(3\text{-dmbpy})](NO_3)$	$P2_1/c$	10.521	9.310	16.570	$\beta=106.6$	4	38
PhHg(CN)phen	$P2_{1/a}$	10.15	18.50	8.86	$\beta=99.59$	4	39
$Hg(CN)_2(PPh_3)_2$	$Pn2_1^a$	18.02	18.26	10.03		4	40
PhHg(meoxine)	$C2/c$	22.961	9.142	16.412	$\beta=127.75$	8	41
PhHg(oxine)	*Pnam*(phase I)	23.12	16.59	6.62		8	41
	$P2_12_12_1$(phase II)	5.584	9.902	23.073		4	41
$[MeHg(py_2CH_2)](NO_3)$	$P2_1/n$	16.875	8.540	9.353	$\beta=96.544$	4	42
$[MeHg(Et_3terpy)](NO_3)$	$P2_1/n$	9.115	15.725	15.566	$\beta=94.465$	4	42

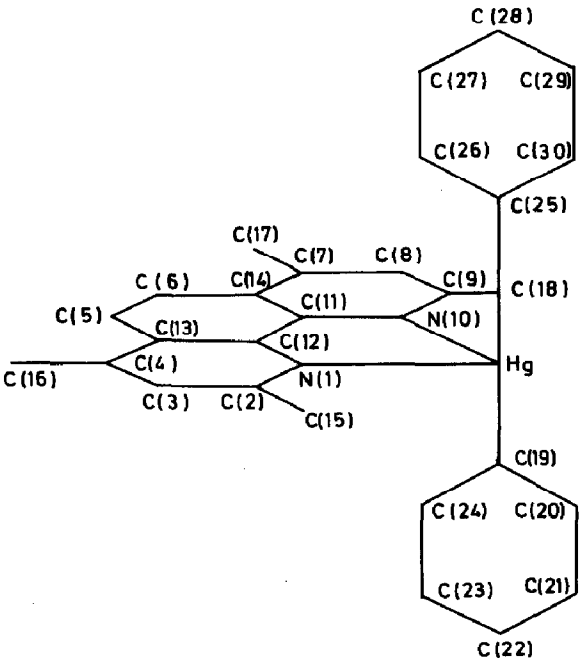

Fig. 1. Atom numbering scheme for $Ph_2Hg(2\text{-tmp})_2$. Adjacent ligand Ph_2Hg moieties in the plane $y = 1/4$ are shown. Adjacent ligand Ph_2Hg moieties in (020) have an atom numbering scheme related by a two-fold axis about the C–Hg–C unit. (Reproduced with permission from Acta Crystallogr., 28B (1972) 1872.)

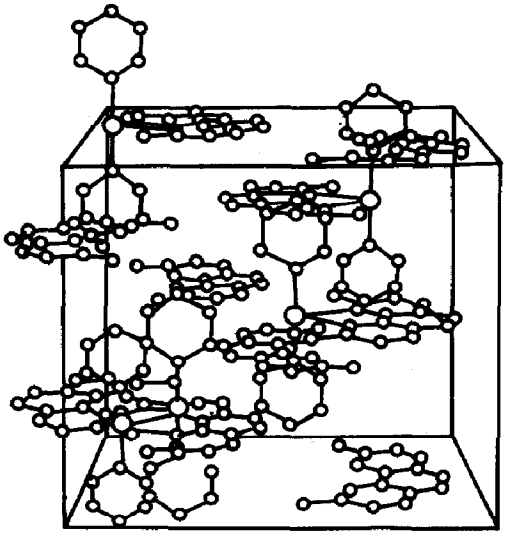

Fig. 2. Stereospecific view of an ordered cell of $Ph_2Hg(2\text{-dmp})_2$ containing a 1:1 complex and an uncoordinated ligand in each (040) plane. (Reproduced with permission from Acta Crystallogr., 28B (1972) 1872.)

possible to ascertain whether the nitrogen atoms are definitely within the sum of Van der Waals radii from Hg (3.0 Å with Hg radius of 1.50 or 3.23 Å with the upper limit of 1.73 Å suggested by Grdenic [43]). Hence the interaction between mercury(II) and nitrogen is weak.

The adducts of symmetrical alkynyl substrates, $(RC{\equiv}C)_2HgL$ (R = Me, $ClCH_2$ and $BrCH_2$; L = phen and 2-dmp), could not be characterized by IR spectroscopy as those of Ph_2Hg [23]. The single crystal X-ray study of $(PhC{\equiv}C)_2Hg(phen)$ shows the complex to be monoclinic with space group $P2_1/n$ (Table 3) [35]. The mercury atom is four coordinate with a practically planar phen molecule, but the geometry is far from tetrahedral. The phen molecule forms an angle of 85.83° with the plane defined by mercury and four carbon atoms of the two acetylenic groups which bond to mercury and to the phenyl groups in a non-linear fashion. The C≡C length appears unaffected by coordination. The C(1)–Hg–C(11) angle (165.6°) and the two Hg–N distances (2.67–2.69 Å) indicate a weak but clear donor–acceptor interaction (Fig. 3) [24].

The adducts $(PhHgC{\equiv}CH)(phen)_2$ and (PhHgC≡CR)phen (R = Me, Ph and $ClCH_2$) have been studied by IR spectroscopy (Table 4) [12]. The $\nu(Hg–C{\equiv})$ peaks occur at lower frequencies than those in the corresponding $(X{\equiv}C)_2Hg$ derivatives, and the reduction is attributed to weakening of the Hg–C≡ bond by the phenyl group. It is, however, difficult to decide if any possible shifts in $\nu(Hg–C_{Ph})$ are due to interference by various ring vibra-

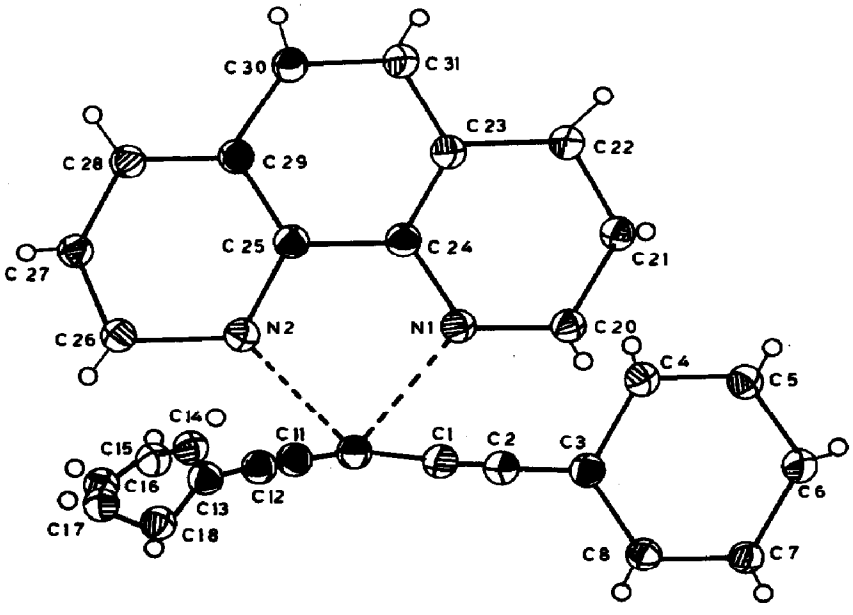

Fig. 3. ORTEP drawing of $Hg(Ph–C{\equiv}C)_2(phen)$. The numbering of the hydrogen atoms (not shown) is that of the carbon atoms to which they are bonded. (Reproduced with permission from Acta Crystallogr., 34B (1978) 3382.)

tions. For instance, the benzene ring with a mercury substituent gives six ring vibrations, namely *q*, *r*, *t*, *u*, *x* and *y* [19,44,45]. The most sensitive to change in X in Ph–Hg–C≡X from the *q*, *r*, and *t* vibrations of ν(Hg–C) is the *t* vibration. In the IR spectra of (Ph–Hg–C≡X)phen compounds, the splitting and shifts in many of the phen bands take place in a fashion similar to those described by Schilt and Taylor [46]. A band of high intensity lies between 230 and 245 cm^{-1} due to the L(C) vibration of the ligand (activated on coordination). A band at 455 cm^{-1} was assigned to the *y* vibration of the Ph of Ph–Hg. The *t* vibration peaks appear in the range 250–270 cm^{-1}. In the IR spectrum of the chloro derivative, the band due to ν(C–Cl) occurs at 680 cm^{-1} (obscured in the starting compound by Ph at 669 cm^{-1}). This shift is probably due to a Hg · · · Cl intermolecular interaction reduced in the adduct. The shift in ν(≡C–H) and splitting of δ(≡C–H) in the adduct could be caused by interaction of the acetylenic hydrogen. The presence of a second molecule of the ligand in this adduct is also in agreement with this supposition.

From the comparative study of $\nu(Hg–C_{Ph})$ (or *t* vibration), ν(Hg–C≡) and ν(C≡C) stretching vibrations, few trends have been noted (Table 5). In many cases, the ν(C≡C) peaks were not observed and the bands due to ν(Hg–C≡) are weak and assignments tentative. However, addition of the ligand leads to little shift in these frequencies. These frequencies are also lower than in the corresponding $(X≡C)_2Hg$ compounds. Nevertheless, in the asymmetric derivatives, the $\nu(Hg–C_{Ph})$ peaks show an upward shift compared with those of Ph_2Hg. It is concluded that the Ph group attached to Hg in (PhHg–C≡X) compounds relaxes the Hg–C≡ bond vis-a-vis the $(X≡C)_2Hg$ compounds, leading to a decrease in the intensity of this band. Simulta-

TABLE 4

The IR data for (PhHgC≡X)phen adducts (cm^{-1}) [a]

Assignment	(PhHgCN)L	(PhHgC≡CH)L_2	(PhHgC≡CCH_3)L	(PhHgC≡CCH_2Cl)L	(PhHgC≡CPh)L
ν(≡C–H)		3265m			
ν(C–Cl)				680s	
δ(≡C–H)		660s			
L	631s	632s, 620sh	623s		625m
y	450w	456w	452s	452s	454m
L(A)	415w	410w	410w	413m	413w
ν(Hg–C≡)	395m	426vw	330w	320w	369vw
t	260w, 250vw	275m	258m, 250m	258s, 245w	253m
L(C)	232w	240w		235w	

[a] All data from ref. 12.

neously, the Lewis acidity of the mercury atom seems to be diminished, probably due to the less polar nature of the Hg–C_{Ph} bond compared with the Hg–C≡ bond. Thus a weak donor–acceptor interaction exists in (Ph-HgC≡X)L and the acceptor capacity is intermediate between that of Ph_2Hg and $(X{\equiv}C)_2Hg$ derivatives.

Complexes of $(C_6F_5)_2Hg$ have been studied to a relatively greater extent than those of (Ph_2Hg) due to the greater Lewis acidity of the fluoro organomercurial. The adducts are of the type: (i) $(C_6F_5)_2HgL$ (L = bpy, phen, dmdp, dmda, dmbpy, 2-tmp, en and opda); (ii) $(C_6F_5)_2HgL$ (L = Ph_3P and Ph_3PO); and (iii) $(C_6F_5)_2HgL_{1/2}$ (L = mdp and mda) (Table 2) [15,17,25,26]. These have been studied mostly by IR, UV, molecular weight and X-ray powder photographic methods. In one case, the single crystal X-ray study has been reported [26]. The X-ray powder diffraction patterns of the adducts did not give much information except indicating that they are new material and not mechanical mixtures of reactants [47–51]. In the IR spectra, the absorption of the free mercurial at 811 cm^{-1} (X-sensitive mode involving ν(Hg–C)) is shifted to low frequencies (784–804 cm^{-1}) in the

TABLE 5

Comparison of ν(Hg–C≡C), t vibration and other vibrations for $(X{\equiv}C)_2Hg$ and (Ph–HgC≡X) and their adducts [a]

Compound	ν(Hg–C≡((cm^{-1})	t vibration (cm^{-1})	ν(C–Cl)
Ph_2Hg		253, 249, 243	
$Hg(CN)_2$	412, 442		
$Hg(CN)_2$(phen)	400, 380		
PhHg(CN)	385	260, 245, 240	
PhHg(CN)(phen)	395	260, 250	
PhHgC≡CH	427	284	
PhHgC≡CH(phen)	426	275	
$(CH_3C{\equiv}C)_2Hg$	381, 360		
$(CH_3C{\equiv}C)_2Hg$(phen)	375, 357		
$PhHgC{\equiv}CCH_3$	340	260, 245	
$PhHgC{\equiv}CCH_3$(phen)	330	258, 250	
$(ClCH_2C{\equiv}C)_2Hg$	366, 358		708
$(ClCH_2C{\equiv}C)_2Hg$(phen)	358		684
$(ClCH_2C{\equiv}C)HgPh$	342	282, 258	
$(ClCH_2C{\equiv}C)HgPh$(phen)	320	258, 245	680
$(PhC{\equiv}C)_2Hg$	379		
$(PhC{\equiv}C)_2Hg$(phen)	369		
(PhHgC≡CPh)	369	253, 243	
(PhHgC≡CPh)(phen)	369	253	

[a] All data from ref. 12.

spectra of the complexes, as expected for a metal–ligand mode with an increase in coordination number [52]. The ν(CC) modes of bpy at 1582 and 1560 cm^{-1}, the ring breathing mode at 992 cm^{-1} and the out-of-plane ring deformation at 403 cm^{-1} are shifted to higher frequencies in the spectrum of $(C_6F_5)_2Hg(bpy)$, as expected for coordinated bpy [46,53–56]. The analogous shifts of 4-dmbpy bands at 1593 amd 993 cm^{-1} to 1609 and 1005 cm^{-1}, respectively, in the spectrum of $(C_6F_5)_2Hg(4\text{-dmbpy})$, presumably indicate coordination of the substituted bpy. Most of the bands of phen in the region 1620–1400 cm^{-1} are displaced to higher frequencies in the spectrum of $(C_6F_5)_2Hg(phen)$ [46,57]. In the complex $(C_6F_5)_2Hg(OPPh_3)$; the ν(P=O) at 1190 cm^{-1} of the free ligand shifts to 1164 cm^{-1}, supporting coordination by Ph_3PO [47–49,58]. The IR spectrum of $(C_6F_5)_2Hg(PPh_3)$ shows a band at 707 cm^{-1} (X-sensitive model r of Ph_3P). The appearance of a separate absorption due to this mode, in contrast to the spectrum of the free ligand, is the most significant characteristic of the coordinated Ph_3P [51]. The absorption bands of $(C_6F_5)_2Hg(en)$ and $(C_6F_5)_2Hg(opda)$ in the region 3450–3150 cm^{-1} are attributable to ν(NH) and are at significantly higher frequencies than the corresponding bands of liquid en and solid opda, respectively [59,60]. These shifts may indicate partial disruption of the intermolecular hydrogen bonding of the free ligands owing to complex formation [59,62–64]. No change in the IR spectra of the other complexes was detected. The UV absorption bands of $(C_6F_5)_2HgL$ (L = bpy, 4-dmbpy) in the region 220–340 nm do not show the shifts to longer wavelengths from free ligand values, normally but not always observed on coordination of bpy or related terpy [34]. Thus, UV spectroscopy has not been useful in the structure eludication of organomercury complexes. Molecular weight data (in benzene or $CHCl_3$) indicate the dissociation of many complexes in solution (Table 6). However, the molecular weight studies show that some derivatives of $(C_6F_5)_2Hg$ with neutral ligands are coordination complexes rather than loose lattice adducts.

The single crystal X-ray study of $(C_6F_5)_2Hg(mda)_{1/2}$ shows that each arsine is coordinated to a mercury atom, yet neither IR nor molecular weight data provide evidence for coordination of the arsine [26]. The adduct is monoclinic with space group *C2/c* (Table 3). It has a two-fold axis about the $-CH_2-$ carbon of the ligand. Each mercury atom has one arsine atom within the sum of Van der Waals radii (HgAs = 3.40 ± 0.2 Å), and there is a T-shaped distribution of two C_6F_5 groups (C–Hg–C angle 173 ± 4°) (Fig. 4). The Hg–As distance is 0.10 Å less than the sum of Van der Waals radii (2.0 Å for As [65,66], 1.5 Å for Hg [43]). However, according to Grdenic [43], an upper limit of 1.73 Å for the radius of mercury can be used as a criterion to indicate some form of bonding. Compared with literature data (Hg–As = 2.60–2.82 Å), the interaction in the present case appears to be very weak [61]. The complex of mdp is isomorphic with that of mda. The complexes

TABLE 6

Molecular weights of some adducts of fluoroorganomercury(II) substrates

Adduct	Molecular weight		Ref.
	Observed	Calculated	
$(C_6F_5)_2Hg(bpy)$	365	691	25
$(C_6F_5)_2Hg(phen)$	673	715	25
$(C_6F_5)_2Hg(dmdp)$	475	933	25
$(C_6F_5)_2Hg(4\text{-}dmbpy)$	420	719	25
$(C_6F_5)_2Hg(2\text{-}tmp)$	604	771	25
$(C_6F_5)_2Hg(en)$	624	595	25
$(C_6F_5)_2Hg(opd)$	333	643	25
$(C_6F_5)_2Hg(PPh_3)$	391	797	25
$(C_6F_5)_2Hg(OPPh_3)$	439	813	25
$(C_6F_5)_2Hg(dmda)$	499	1021	25
$(CF_3)_2Hg(phen)$	516	519	29
$(C_2F_5)_2Hg(phen)$	616	619	29
$(C_3F_7)_2Hg(phen)$	695	719	29
$(CF_3)_2Hg(bpy)$	395	495	29
$(C_2F_5)_2Hg(bpy)$	568	595	29
$(C_3F_7)_2Hg(bpy)$	647	695	29

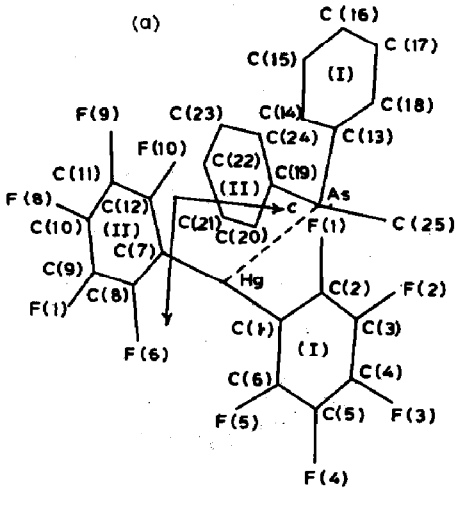

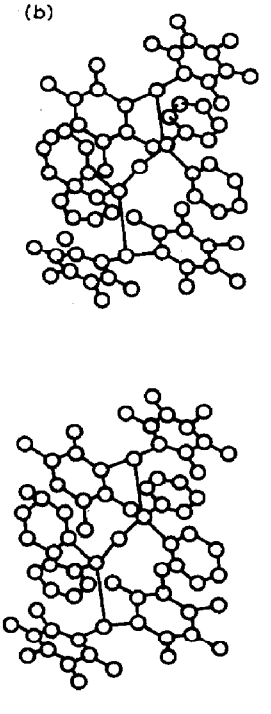

Fig. 4(a). A drawing of the asymmetric unit $(C_6F_5)_2Hg(mda)_{1/2}$, showing the atom numbering scheme. (Reproduced with permission from J. Chem. Soc., Dalton Trans., (1972) 511.)

Fig. 4(b). Stereospecific view of $(C_6F_5)_2Hg(mda)_{1/2}$ along the (010) direction, showing the two-fold axis. (Reproduced with permission from J. Chem. Soc., Dalton Trans., (1972) 511.)

with Ph_3P and Ph_3PO have three-coordinate Hg and the stereochemistry may be distorted from trigonal planar towards T-shaped owing to the stability of the linear C–Hg–C arrangement [43,67,68]. However, further investigation is needed to determine the structures of complexes of Ph_3P, Ph_3PO, dmdp and dmda.

Whereas dialkylmercurial systems (or related systems) do not interact with ligands, the corresponding fluoro- or chloro-alkyl- or alkenyl-organomercury(II) derivatives form a number of adducts due to their enhanced Lewis acidity (Table 2) [29–31]. The characterization is mainly through IR, ^1H NMR, ^{35}Cl NQR, molecular weight and mass spectral data. The IR spectra of the adducts $(R_f)_2HgL$ ($R_f = CF_3$, C_2F_5 and C_3F_7; L = phen and bpy) reveal absorption due to perfluoroalkyl groups in the expected range of 1350–800 cm^{-1} [69–73]. The ligands show their usual behaviour indicative of coordination [46]. The phen adducts are monomers (in benzene), but the molecular weights of the bpy adducts are less than calculated and dissociation into parent organomercurial and ligand occurs (Table 6). Hence, the phen complexes are more stable in terms of dissociation than the corresponding bpy complexes [15,17,25]. The relative stability of the bpy complexes appears to be: $(C_2F_5)_2Hg(bpy) \geq (C_3F_7)_2(bpy) > (CF_3)_2Hg(bpy) > (C_6F_5)_2Hg(bpy)$. However, the stability differences do not necessarily imply differences in the Hg–N bond strengths, but may be due to variations in the solvation energies of the free mercurials or in the entropies of formation of the complexes.

In the solution phase IR spectroscopic study of the interaction of the ligand en with $(CF_3)_2Hg$, $[(CF_3)_2CF]_2Hg$, etc., in CCl_4, no significant change occurs in the position of the NH stretching frequencies (3395–3400; 3315–3330 cm^{-1}) from that of free en (3395, 3310 cm^{-1}) [1 : 1 mole ratio mixture of en and the bis(fluoroalkyl) mercurials]. However, the δ(N–H) mode decreases from 1620 cm^{-1} in the solution of en to 1582–1590 cm^{-1} in the solution of the mixture. Significantly, the ν(N–H) peaks are very sharp in the mixtures compared with free en—a feature associated with hydrogen bonding. These changes in the IR spectra are consistent with the disruption of intermolecular hydrogen bonds brought about by formation of relatively weak coordination compounds. The IR spectra of 1 : 1 and 1 : 2 mole ratio (metal : ligand) mixtures of C_4H_8SO and bis(fluoroalkyl) mercurials show that the position of ν(SO) at 1036 cm^{-1} in free C_4H_8SO is shifted to 1016–1023 cm^{-1} in the complexes. The decrease is however nearly the same for both mole ratios. The 1 : 3 mole ratio merely gave the additional absorption band of the ligand. Hence, the IR spectroscopic data clearly show the formation of three- and four-coordinate adducts by C_4H_8SO. Two complexes, $(CF_3CHF)_2Hg(OSC_4H_8)_2$ and $(CF_3CH_2)_2Hg(en)$, can be isolated.

Bis(trichlorovinyl)mercury, a stronger Lewis acid than Ph_2Hg, but weaker than $(C_6F_5)_2Hg$, is the first bis(alkenyl) mercurial forming complexes of the type $(Cl_3C_2)_2HgL$ (L = phen, 2-dmp, 3-tmp, bpy and dmdp) [32]. In the IR spectra of the complexes, the absorption of the free mercurial at 828 cm^{-1} is shifted significantly to lower frequencies, as expected for a metal–ligand mode with increase in coordination number. The ν(C=C) mode of bpy at

TABLE 7

^1H NMR and ^{35}Cl NQR data for ligands and their adducts with $(Cl_3C_2)_2Hg$

	L (ppm)	$(Cl_3C_2)_2HgL$ (ppm)	Ref.
^1H NMR data [a]			
I (solid state)			
phen	7.64, 7.72, 7.81, 8.28, 8.40	7.75, 7.82, 7.90, 7.97 8.38, 8.30	32
bpy	7.22, 7.35, 7.42, 7.75, 7.88, 8.01, 8.62, 8.76, 8.85	7.33, 7.45, 7.53, 7.81 7.95, 8.07, 8.48, 8.82, 8.90	32
2-dmp	2.96, 7.48, 7.62, 7.76, 8.13, 8.27	3.05, 7.61, 7.75, 7.86, 8.29, 8.43	32
3-tmp	2.58, 2.70, 8.08	2.67, 2.76, 8.17	32
dmdp	2.00, 2.07, 2.14, 7.41	2.11, 2.18, 2.25, 7.48	32
II (solution phase) 1 : 1 mixture			
Ph_3P	7.37, 7.42	7.42, 7.47	32
py	7.23, 7.29, 7.34, 7.43, 7.61, 7.74, 8.71, 8.76	7.30, 7.35, 7.39, 7.49, 7.68, 7.81, 8.76, 8.81	32
thiophene	7.12, 7.18, 7.34, 7.37	7.17, 7.26, 7.40, 7.44	32
tmed	2.21, 2.34, 7.37, 7.42	2.27, 2.40, 7.42, 7.47	32
^{35}Cl NQR	Frequencies (MHz)		
	77 K	293 K	
$(Cl_3C_2)_2Hg$	35.42, 35.59, 36.15, 36.89, 37.30 [b]		74
$(Cl_3C_2)_2Hg$(2-dmp)	34.74, 34.87, 36.28, 36.68, 37.03, 37.14	34.03, 34.215, 35.40, 35.645, 35.88, 35.965	32
$(Cl_3C_2)_2Hg$(3-tmp)	35.21, 35.38, 36.25 [b], 36.97, 37.15	35.39, 35.71, 36.42 [c]	32

[a] Reference standard for ^1H NMR is TMS and solvent CCl_4.

[b] Double intensity.

[b] Incomplete spectrum.

1582 and 1560 cm^{-1}, and the ring breathing mode at 992 cm^{-1}, are shifted to higher frequencies (1592, 1570 and 1005 cm^{-1}, respectively) on coordination. Similarly, most of the bands associated with phen, 2-dmp and 3-tmp in the 1350–1620 cm^{-1} region are displaced to higher frequencies on coordination. The most significant features in the spectrum of $(Cl_3C_2)_2Hg$(dmdp) are the presence of strong bands at 822 and 1550 cm^{-1}, both absent in the spectrum of the free ligand. The downward shifts observed in the ^1H NMR spectra of the complexes indicate weak interaction of the ligands with the chloromercurial compared with that observed for mercury(II) chloride complexes (Table 7). ^1H NMR data show very weak interaction of Ph_3P, pyridine, thiophene and tmed with the mercurial in the solution phase.

The most significant feature of the ^{35}Cl NQR data for $(Cl_3C_2)_2Hg$(2-dmp) and $(Cl_3C_2)_2Hg$(3-tmp) (Table 7), is the reduction in frequency of the two lowest frequency resonances on complex formation. Generally, an increase in charge on chlorine corresponds to reduction in NQR frequency assuming other effects are constant [75]. These two resonances may be reasonably ascribed to the α-chlorine atoms by comparison with the NQR spectrum of $(Cl_2C{=}CCl)HgCl$, in which the α-chlorine resonance (35.42 MHz) is 1.93 MHz lower than the average of the β-chlorine resonances (37.56 and 37.13 MHz) [76]. The reduction in frequency upon complex formation is greater for the 2-dmp complex (0.70 MHz) than for the 3-tmp complex (0.21 MHz), suggesting a greater degree of charge transfer in the 2-dmp complex; this is further supported by thermal studies. However, there is little difference in the frequency shift averaged over all the chlorine atoms (0.37 MHz for the 2-dmp and 0.45 MHz for the 3-tmp complex). This amounts to about a one percent change in average chlorine charge. The multiplicity of the NQR spectrum for the 2-dmp complex indicates the presence of six crystallographically inequivalent chlorine atoms, whereas for the 3-tmp complex only five lines were observed, one of which is of double intensity, doubtless corresponding to two similarly bonded chlorine atoms.

It is obvious from Table 8 that the thermal stability of the bidentate nitrogen complexes, $(Cl_3C_2)_2HgL$, increases in the order L = bpy, phen, 2-dmp, 3-tmp. The greater stability of the phen complex compared with that of bpy is in agreement with earlier work on organomercurials [21,29,77]. The relative stabilities have been ascribed to the tendency of organomercurials to preserve approximate linearity upon coordination, thus necessitating the approaching ligands to interact with *p* orbitals on mercury. The planar phen ligand could give reasonable overlap with these mercury *p* orbitals, whereas bpy is twisted to minimize interaction of the 3,3′-hydrogen atoms, leading to poorer overlap and hence weaker mercury–ligand interactions. In fact, $(Cl_3C_2)_2Hg$(bpy) is an extremely weak complex in the solid state because its melting point and thermal behaviour are very similar to that of the parent

mercurial. However, the small yet significant difference between IR and NMR spectra of this product compared with the free mercurial and bpy support the formulation as a loose lattice adduct. The residue in both the substituted phen complexes may be due to C_4Cl_4, but this is doubtless polymeric since it does not show any mass spectral features. The pattern of decomposition appears to be

$$n(Cl_3C_2)_2HgL \rightarrow nL + nHgCl_2 + (C_4Cl_4)_n \quad (L = dmp, tmp)$$

The complex $(Cl_3C_2)_2Hg(dmdp)$ appears to have comparable thermal stability, but no thermally stable intermediate could be detected in its thermogram.

(ii) Adducts of aryl- or alkyl-mercuryl(II) halides or pseudohalides and their fluoro derivatives

Various adducts reported with this class of organomercurials, together with the techniques used for their study are given in Table 9.

The adducts of oxines or substituted oxines have been well characterized [41,78]. The UV–VIS spectra of all RHg(oxine) adducts in solution and in the solid state show intense broad absorption at 365–380 nm (Table 10)

TABLE 8

Thermal characteristics [a] of $(Cl_3C_2)_2Hg$ and its 1:1 adducts with phen, bpy, 2-dmp, 3-tmp and dmdp

Compound	L	Temperature (°C)	Thermal behaviour
$(Cl_3C_2)_2Hg$	100	Sublimation begins	
	205	Mass loss complete	
$(Cl_3C_2)_2HgL$	bpy	75–190	Single step mass loss, 2% residue
	phen	150	Onset of mass loss
		225–400	45.6% mass loss
		400–800	13.3% residue
	2-dmp	175	Mass loss begins
		175–420	Complex thermogram (inclusive)
		420–650	28.1% residue (C_4Cl_4)
	3-tmp	200	Mass loss begins
		200–230	30.3% loss (3-tmp)
		230–320	43.3% loss ($HgCl_2$)
		320–600	residue (C_4Cl_4)
	dmdp	140	Onset of mass loss
		550	Complete mass loss

[a] All data from ref. 32.

attributable to the ^1L_a transition [90] shifted to longer wavelengths from its position in oxine (315 nm) [91–93] or 8-methoxyquinoline (297 nm) [94], as expected for chelated oxines [92,93,95–99]. Similar shifts are observed for RHg(meoxine) complexes. For unidentate O-bonded complexes, the ^1L_a band is near the free ligand position [92,96,98]. For the systems RHg(oxine) (R = Ph, Me, p-HC_6F_4 or p-$MeOC_6F_4$), the extinction coefficients are lower in ethanol than in other solvents, unlike the chelated transition metal oxine complexes having similar extinction coefficients in both ethanol and chloroform [46]. The difference may be attributed to displacement of nitrogen by ethanol.

The molecular weights of the complexes RHg(oxine) (R = C_6F_5, p-HC_6F_4, p-$MeOC_6F_4$ or Ph) and RHg(meoxine) (R = Me or Ph) are higher than monomeric values and increase with increasing concentration, consistent

TABLE 9

Adducts of unsymmetrical organomercury(II) derivatives

Adduct	Ligand (L)	Techniques	Ref.
1. (a) RHg(oxine) (R = C_6F_5, p-HC_6F_4, p-$MeOC_6H_4$)	oxines	mol. wt., X-ray, UV and mass	78
(b) PhHg(oxine), PhHg(meoxine), MeHg(oxine)·H_2O, MeHg(meoxine)	oxines	mol. wt., X-ray, UV and mass	78
2. (a) $(C_6F_5HgX)L$ (X = Cl, Br)	bpy, phen, 3-tmp, 2-dmp	IR and mol. wt.	77, 79, 80
(b) $(C_6Cl_5HgCl)L$	phen, 2-dmp, 3-tmp	IR and mol. wt.	77, 79, 80
3. (PhHgCl)L	phen, 3-tmp	IR and X-ray	81
4. (a) $(MeHgCl)_2L$	N–N [a]	^1H NMR	82
(b) (MeHgCl)L	N–N [a]	^1H NMR	82
5. (a) [RHgL]X	R, L, X [b]	IR	83, 84
(b) $[PhHgPEt_3](NO_3)$		IR	85
6. $(C_2Cl_3)HgXL$	L [c]	^1H NMR, IR and mass	86
7. (a) $[MeHgL](NO_3)$	L [d]	IR and ^1H, ^{13}C and ^{199}Hg NMR	36, 37, 87–89
(b) $[MeHgL_{1/2}](NO_3)$	3-dmbpy	IR, ^1H, ^{13}C, ^{199}Hg NMR and X-ray	36, 38
(c) $[MeHgL](NO_3)$	bpy	X-ray	36
(d) $[MeHgL](NO_3)$	L [e]	^1H NMR and X-ray	42, 90

[a] N–N = $H_2N(CH_2)_3NH_2$ or $H_2N(CH_2)_4NH_2$.

[b] R = Me, Et, n-Pr, n-Bu; X = Cl, Br, I, ClO_4, BF_4, $Cr(NH_3)_2(SCN)_4$; L = PMe_3, PEt_3, PPh_3, $PPhMe_2$, $AsPh_3$, $AsEt_3$.

[c] L = phen, 2-dmp, 3-tmp, bpy, tmed.

[d] L = bpy, 3-dmbpy, 4-dmbpy, 5-dmbpy, 6-dmbpy, 2-dmp, 4-dmp, 5-dmp.

[e] L = terpy, Et_3terpy, py_2CMe_2, py_2CEt_2, py_3CH.

with partial dimerization of the molecules in solution (Tables 11 and 12). The dimerization implies that the compounds have associated structures in the solid state. The dimerization appears to be more extensive in CCl_4 than

TABLE 10

UV–VIS spectra of organomercuric quinolin-8-olates and 2-methylquinolin-8-olates in various media

Complex	λ_{max} (log ε) (nm)	Complex	λ_{max} (log ε) (nm)	Ref.
C_6F_5Hg(oxine)		PhHg(oxine)		
nujol	370	nujol	334sh, 380	78
$CHCl_3$	369(3.44)	CCl_4	336sh, 379(3.48)	
		$CHCl_3$	369(3.41)	
		C_6H_6	336sh, 376(3.48)	
p-HC_6F_4Hg(oxine)		C_6H_{14}	335sh, 379(3.36)	
nujol	370			
$CHCl_3$	369(3.09)	EtOH	338(2.98), 378(2.94)	
EtOH	338sh, 378(2.91)	PhHg(meoxine)		
		$CHCl_3$	361(3.20)	
p-$MeOC_6F_4Hg$(oxine)				
nujol	370	MeHg(meoxine)		
$CHCl_3$	369(3.86)	$CHCl_3$	359(3.28)	
EtOH	338sh, 378(3.26)	H(oxine)		
		$CHCl_3$	314 free ligand	
MeHg(oxine)				
nujol	334sh, 380	H(meoxine)		
$CHCl_3$	369(3.30)	$CHCl_3$	320 free ligand	
EtOH	338(2.51), 378(2.43)			
MeHg(oxine)H_2O				
nujol	334sh, 380			

TABLE 11

Molecular weights of the oxine complexes [a]

Complex	Found			Expected
	C_6H_6	$CHCl_3$	CCl_4	
C_6F_5Hg(oxine)	583	557		512
p-$MeOC_6F_4Hg$(oxine)	561	558	645	524
p-HC_6F_4Hg(oxine)	526	536		494
PhHg(oxine)	451		480	422
MeHg(oxine)	395			378
PhHg(meoxine)	469		531	436
MeHg(meoxine)	450			374

[a] All data from ref. 78.

in benzene or $CHCl_3$, and more extensive for meoxine complexes than for oxine complexes. The complexes MeHg(oxine) and MeHg(oxine)H_2O are essentially monomeric and the values for the latter are higher than those for the former, suggesting that water remains bonded in solution, probably hydrogen bonded to quinolin-8-olate oxygen. In the mass spectra of the oxine complexes, in addition to intense monomer parent ions, the complexes RHg(oxine) (R = *p*-HC_4F_4, *p*-$MeOC_6F_4$ or Ph) and RHg(meoxine) (R = Ph, Me) showed low intensity clusters attributable to $(RHg)_2$(oxine or meoxine) (Table 13) which may arise from breakdown of undetected dimer parent ions. This again indicates that the complexes may be partly dimeric in the vapour state implying associated solid-state structures. The complexes C_6F_5Hg(oxine) or MeHg(oxine)H_2O showed only monomer parent ions. Hence, all RHg(oxine or meoxine) complexes, except for MeHg(oxine) and MeHg(oxine)H_2O, are partially dimeric in solution and have associated structures in the solid state.

The crystal structure of PhHg(meoxine) shows that its crystals are monoclinic, *C2/c* [41]. The complex PhHg(oxine) has two phases: phase I is orthorhombic with space group *Pnam*, whereas phase II is orthorhombic with space group $P2_12_12_1$ (Table 3) (Figs. 5–8). In spite of their apparent similarity, the three structures determined show a variation which is subtle and interesting. In the complex PhHg(meoxine) the unit cell contents comprise associations of pairs of molecules linked about the crystallographic two-fold axes by Hg · · · O interactions, leading to the formation of dimers with intrinsic symmetry of 2 (Fig. 5). The interactions between different dimers are not significant. The meoxine ligand is approximately planar, and coplanar with the mercury, while the phenyl ring is approximately normal to it. In phase I, two independent molecules occur within the structure. The oxine ligands, together with the associated mercury atoms, lie in the mirror

TABLE 12

The equilibrium constants [a] for dimerization of RHgL(oxine) or RHg(meoxine) complexes

Complex	Equilibrium constant			Complex	Equilibrium constant	
	C_6H_6	$CHCl_3$	CCl_4		C_6H_6	CCl_4
C_6F_5Hg(oxine)	9.8	4.7		MeHg(oxine)H_2O	monomeric	
p-HC_6F_4Hg(oxine)	8.0	10		MeHg(oxine)	monmeric	
p-$MeOC_6F_4$(oxine)	3.6	8.0	34	PhHg(meoxine)	4.5	27
PhHg(oxine)	3.5	1.0	8.6	MeHg(meoxine)	21	

[a] All data from ref. 78.

TABLE 13

Mass spectral data [a] for RHg(oxine) or RHg(meoxine) complexes

Compound	*m/e*	Assignment	Compound	*m/e*	Assignment
$C_6F_5Hg(oxine)$	513	$C_6F_5Hg(oxine)^+$	PhHg(oxine)	700	$(PhHg)_2(oxine)^+$
				423	$PhHg(oxine)^+$
$p\text{-}HC_6F_4Hg(oxine)$	844	$(p\text{-}HC_6F_4Hg)_2(oxine)^+$	PhHg(meoxine)	714	$(PhHg)_2(meoxine)^+$
	495	$p\text{-}HC_6F_4Hg(oxine)^+$		437	$PhHg(meoxine)^+$
$p\text{-}MeOC_6F_4Hg(oxine)$	904	$(p\text{-}MeOC_6F_4Hg)_2(oxine)^+$	MeHg(meoxine)	590	$(MeHg)_2(meoxine)^+$
	525	$p\text{-}MeOC_6F_4Hg(oxine)^+$		375	$MeHg(meoxine)^+$
$MeHg(oxine)H_2O$	361	$MeHg(oxine)^+$.			

[a] All data from ref. 78.

planes (Fig. 6) and are thus rigorously planar. The phenyl ring is normal to the ligand plane as in the first case. The molecular packing of this independent pair of molecules resembles that of PhHg(meoxine) in that the Hg · · · O interactions occur between adjacent molecules along *c* and the oxide planes are parallel to each other. There is not an array of dimers, but instead an infinite polymer along *c* comprising a multiple sandwich of alternating molecules *a* and *b*. In phase II, the intermolecular interactions in the lattice

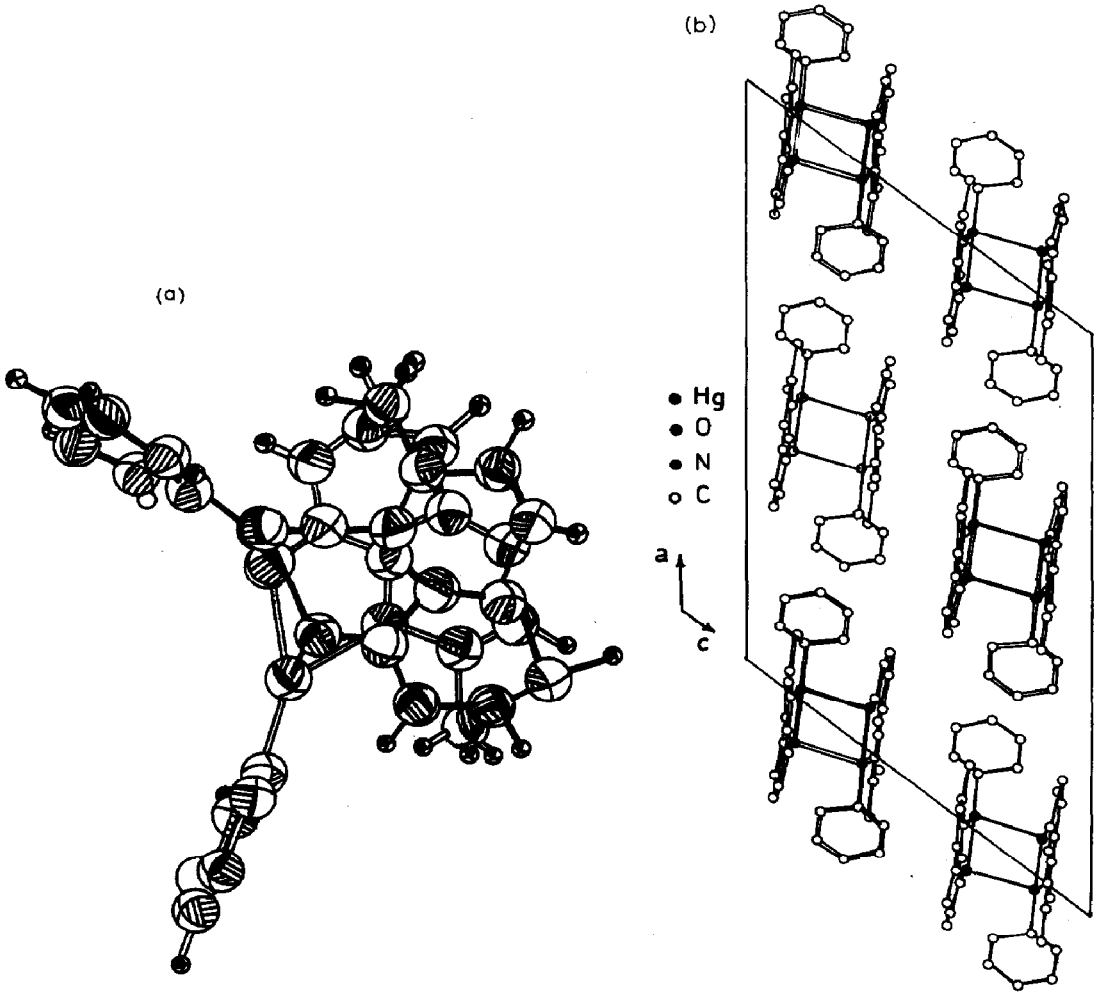

Fig. 5(a). A stereoscopic view of the dimer of PhHg(meoxine) projected normal to the plane of the ligand, displaying the relative disposition of the two molecules. (Reproduced with permission from Aust. J. Chem., 31 (1978) 537.)

Fig. 5(b). Unit cell contents of PhHg(meoxine) projected approximately parallel to the ligand plane (i.e. along *b*) showing the interplanar, intermolecular interactions within the dimer. (Reproduced with permission from Aust. J. Chem., 31 (1978) 537.)

are again dominated by Hg · · · O attractions (Fig. 7). In this case the planes of adjacent molecules do not pack parallel to each other as in the first two cases, but are disposed on the perimeter of the Hg · · · O · · · Hg · · · O helix. The phenyl ring is coplanar with the oxinate ligand. In the first case the Hg · · · O interaction is the shortest observed (2.79 Å), whereas the other two complexes have two Hg · · · O interactions (3.33–3.37 Å) which are very long. In all the complexes, the angle O–Hg–N remains substantially constant at ca. 73° (Fig. 8). In going from the first to the third case, the disposition of the phenyl group changes the angle relative to Hg–O, increasing from 151.8 to 175.0. The Hg–C distance is constant, whereas the Hg–N distance increases considerably on passing from the first to the third case (i.e. from 2.36 to 2.57 Å), while the Hg–O distance decreases from 2.16 to 2.06 Å. Hence, the stereochemistry of the CHg(ON) skeleton varies from pseudo-trigonal to approximately T-shaped.

The organomercurials PhHgCl, $(C_6F_5)HgX$ and $(C_6Cl_5)HgX$ (X = Cl, Br) form 1 : 1 adducts with phen, 2-dmp, 3-tmp amd bpy [77,79–81]. X-ray powder photography reveals that the adducts are not merely mechanical mixtures of reactants. All the adducts, with the exception of $(C_6Cl_5)HgClL$

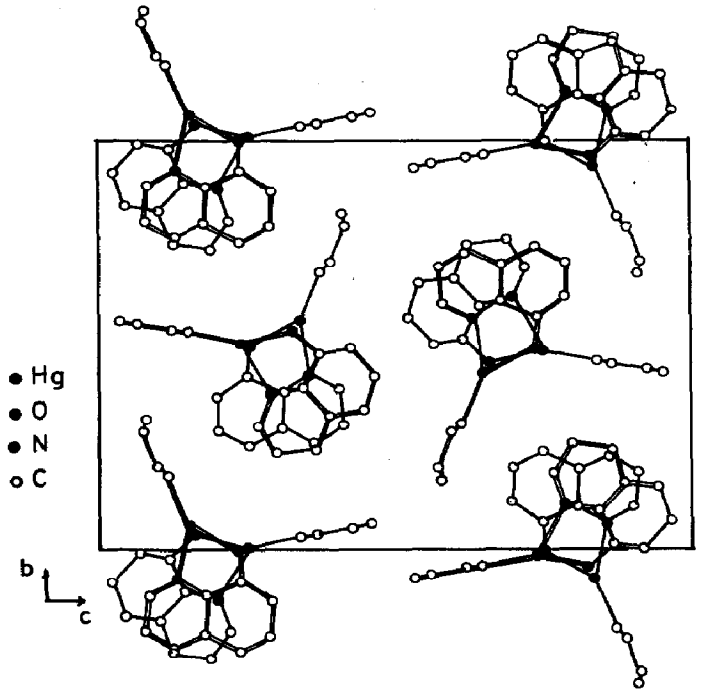

Fig. 6. Unit cell contents of phase I [PhHg(oxine)], projected along *c* (i.e. normal to the ligand planes), showing the interactions between adjacent molecules and their relative disposition. (Reproduced with permission from Aust. J. Chem., 31 (1978) 537.)

(L = phen, 2-dmp) and PhHgCl(3-tmp), undergo complete or partial disproportionation reactions in boiling benzene ($2RHgXL \rightarrow LHgX_2 + R_2HgL$ or $R_2Hg + L$). Nevertheless, the adducts $C_6F_5HgX(2\text{-dmp})$ are monomeric in

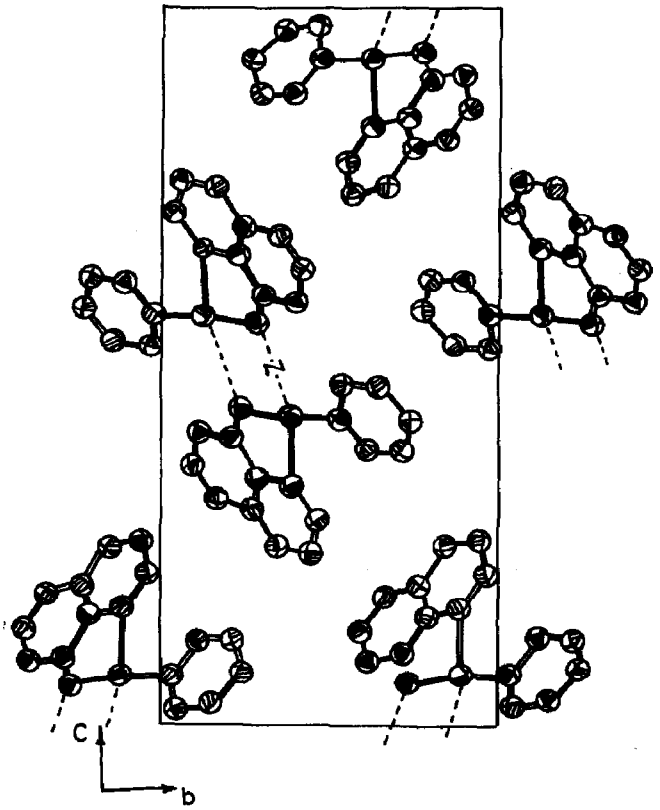

Fig. 7. Unit cell contents of phase II of PhHg(oxine) projected along *a*; intermolecular Hg · · · O contacts are shown by broken lines; 50% thermal ellipsoids are displayed. (Reproduced with permission from Aust. J. Chem., 31 (1978) 537.)

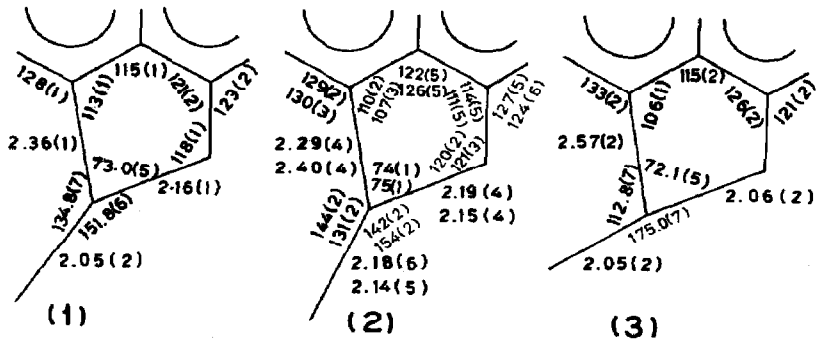

Fig. 8. Geometries about the mercury atom in the plane of the ligand for each compound. (Reproduced with permission from Aust. J. Chem., 31 (1978) 537.)

CH_3COCH_3. The absorptions due to the organic groups and ligands in the range 2000–200cm^{-1} show the usual features. All the chloro complexes, except C_6Cl_5HgCl(3-tmp), show broad intense absorption bands due to ν(Hg–Cl) (Table 14). The ν(Hg–Cl) values of the majority of the chloro complexes are near the values for known mercury(II) chloride complexes (e.g. $HgCl_4^{2-}$, $(Ph_3P)_2HgCl_2$). The lowering of ν(Hg–Cl) on coordination is less marked for PhHgCl · phen and PhHgCl · (3-tmp) than for the other chloro complexes, suggesting that the Hg–Cl bonding is stronger, and hence the Hg–ligand bonding weaker, in the phenyl derivative than in the other RHgClL complexes [52]. This shows that the Lewis acidity of PhHgCl is less than that of $(C_6F_5)HgCl$ or $(C_6Cl_5)HgCl$ [100]. The chloro complexes probably have tetrahedral structures.

The interaction of MeHgCl with $H_2N(CH_2)_3NH_2$(3-pn) and H_2N-$(CH_2)_4NH_2$(bn) has been studied by ^{1}H NMR spectroscopy (Tables 9 and 15) [82]. The ligand protons in the adducts show low-field and methyl protons up-field shifts. This shows a shift in the electron density from nitrogen to mercury via σ-type bonding. In the 1 : 1 mixture of $H_2N(CH_2)_3NH_2$ and MeHgCl, the proton chemical shifts revealed the formation of both 1 : 1 and 2 : 1 (metal : ligand) complexes in the 1 : 1 mixture. The α- and β-protons of the free ligand showed the typical triplet and quintet forms, respectively, reflecting the bilateral symmetry of the molecules. In the isolated 2 : 1 adducts of both ligands, the proton signal was the same as for the ligands. Accordingly, structure (A) is assumed for the 2 : 1 complexes of both ligands. The α- and β-proton signals in the 1 : 1 complex of 3-pn also showed triplet and quintet splittings, suggesting either structure (B) or a polymeric structure (C). However, the α- and β-proton

TABLE 14

The ν(Hg–Cl) peaks of RHgCl · L and related complexes [a]

Compound	ν(Hg–Cl) (cm^{-1})	Compound	ν(Hg–Cl) (cm^{-1})
C_6F_5HgCl(bpy)	252s(vbr)	C_6F_5HgCl	344s
C_6F_5HgCl(phen)	239s(br)	C_6Cl_5HgCl	357vs
C_6F_5HgCl(3-tmp)	236s(vbr)	PhHgCl	331s
C_6F_5HgCl(2-dmp)	245s(vbr)	$HgCl_2$bpy	273s(br)
C_6Cl_5HgCl(phen)	263vs(br)	$HgBr_2$phen	272s(br), 242s(br)
C_6Cl_5HgCl(2-dmp)	244s(vbr)	$HgCl_2$(3-tmp)	270vs(vbr)
C_6Cl_5HgCl(3-tmp)	< 220	$HgCl_2$(2-dmp)	280s(vbr), 262s(vbr)
PhHgCl(phen)	314s(br)		
PhHgCl(3-tmp)	293s(br)		

[a] All data from refs. 77 and 79–81.

signals of the 1 : 1 bn complex, did not show the typical splitting pattern clearly. This observation, and particularly a splitting of the α-proton peak, suggests overlap of signals of two different chemical shifts. For the 1 : 1 bn complex, therefore, non-chelate coordination (D) seems to be reasonable, and the chelate structure (B) is preferred over the polymeric structure (C) for the 1 : 1 3-pn complex.

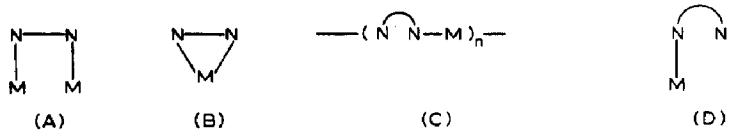

The adducts of alkylmercury halides, $(RHgP'R_3)X$, have not been intensively studied [83–85]. The adducts are not stable and gradually decompose at room temperature over a period of weeks, even when stored under nitrogen. No complex with Ph_3P has been isolated. For arylmercury(II) only one complex has been reported: $[PhHg(PEt_3)](NO_3)$.

The trichlorovinylmercury halide adducts, $(Cl_2C{=}CCl)HgXL$ (X = Cl, Br; L = phen, 2-dmp, 3-tmp, bpy and tmed), have been studied by ^1H NMR, IR and mass spectroscopy (Table 9) [86]. The mass spectral data show that the adducts dissociate even at low bombarding voltage and the spectra were similar to those of the free organomercury halides. The ions correspond to RHg^+ mass. In the IR, strong absorptions due to mercurials at 1542 and 850 cm^{-1} move to the low-energy region, as expected for an increase in coordi-

TABLE 15

^1H NMR data for methylmercury(II)–diamine complexes [a,b]

Compound	$\overset{\gamma}{N}H_2\overset{\gamma}{C}H_2(\overset{\beta}{C}H_2)_m\overset{\alpha}{C}H_2NH_2$–HgMe ($m$ = 1,2)			
	$\Delta\nu_\alpha$ (Hz)	$\Delta\nu_\beta$ (Hz)	$\Delta\nu_\gamma$ (Hz)	$J(^{199}Hg–^1H)$ (Hz)
MeHgL	−25.0	−22.3	4.2	212.0
$(MeHg)_2L$	−29.5	−27.7	3.6	213.0
(MeHgL)(mixture) [c]	−26.7	−23.9	3.8	212.2
L	0	0		
MeHgL′	−24.9	−14.5	4.3	209.8
$(MeHg)_2L'$	−29.5	−16.5	4.6	211.4
L′	0	0		
MeHg			0	221.0

[a] A negative sign indicates downward shift of a proton signal on complex formation.

[b] All data from ref. 82.

[c] Metal and ligands were mixed in 1 : 1 molar ratio in D_2O. L = $NH_2CH_2CH_2CH_2NH_2$(3-pn) and L′ = $H_2NCH_2CH_2CH_2CH_2NH_2$(bn).

nation number. The ν(CC), ring breathing mode and the very intense broad band (756 cm^{-1}) of bpy are shifted to higher frequencies, as expected for the coordinated ligand. In the case of the tmed ligand, the peak at 1265 cm^{-1} shifts to higher frequency and the peaks in the region 850–1000 cm^{-1} increase in intensity. The phen ligand and its analogs show their characteristic behaviour in the range 1300–1600 cm^{-1}. The soluble complexes record downward shifts of the order 0.1–0.2 ppm for the ligand protons, pointing to the movement of electron density from the ligands towards the mercury atom (Table 16). For $(C_2Cl_3)HgX(3\text{-tmp})$ (X = Cl, Br) complexes, the ^1H NMR shifts of the ligand are similar to those found for $(C_2Cl_3)_2Hg(3\text{-tmp})$ and the onset of mass loss occurs at a similar temperature. Thus, both complexes have similar stability. Comparison of the other complexes shows that C_2Cl_3HgX have greater acceptor character than with $(C_2Cl_3)_2Hg$. This is confirmed by thermal studies, where onset of mass loss occurs at higher temperatures for C_2Cl_3HgX than for $(C_2Cl_3)_2Hg$ complexes [32]. The adducts of C_2Cl_3HgX with phen and bpy, as well as $C_2Cl_3HgCl(tmed)$, volatilize in a single step, in some cases leaving a slight residue, doubtless from thermal degradation of the complexes. The t.g.a. of $(C_2Cl_3)HgBr$ and both phen adducts indicate the formation of intermediates derived from the C_2Cl_3 moiety. For example, the adduct $(C_2Cl_3)Hg(3\text{-tmp})$ loses a ligand in the 190–240°C range and $HgCl_2$ in the 240–250°C range, leaving a residue of composition $(C_2Cl_3)_n$ which slowly vaporizes up to 700°C. These studies lead to the conclusion that the substrates C_2Cl_3HgX are weaker acceptors than $(C(NO_2)_3)_2Hg$ and $(C_6F_5)_2Hg$, but stronger than PhHgX (X = Cl, Br).

TABLE 16

^1H NMR spectral data for ligands and their complexes with C_2Cl_3HgX [a,b,c]

L (ppm)	$(C_2Cl_3HgCl)L$ (ppm)	$(C_2Cl_3HgBr)L$ (ppm)
2-dmp 2.98, 7.47, 7.61, 7.75, 8.25	3.10, 7.66, 7.78, 7.87, 8.31, 8.45	3.15, 7.71, 7.86, 7.93, 8.38, 8.52
3-tmp 2.56, 2.69, 8.07, 8.99	2.59, 2.76, 8.15, 8.85	2.59, 2.76, 8.15, 8.84
bpy 7.41, 7.48, 7.51, 7.54, 7.63, 7.88, 7.90, 8.00, 8.13, 8.15, 8.41, 8.43, 8.54, 8.73, 8.82		7.31, 7.60, 7.71, 7.80, 8.05, 8.07, 8.19, 8.20, 8.29, 8.31, 8.54, 8.68, 8.81
tmed 2.27, 2.41	2.48, 2.58	2.48, 2.58

[a] Spectra in $CDCl_3$ (TMS as internal standard).

[b] $(C_2Cl_3)HgXL$ (X = Cl, Br, L = phen; X = Cl, L = bpy) insoluble in $CDCl_3$.

[c] All data from ref. 86.

It may be worth mentioning that reactions with phosphines, Ph_3P, dmdp did not form the desired adducts, but led to symmetrization of the organomercury(II) moiety forming HgX_2–phosphine adducts.

The organomercurial, $MeHgNO_3$, is one of the most studied organomercury systems, and a number of complexes with bipyridines, phenanthrolines and related ligands have been characterized by IR, ^1H, ^{13}C and ^{199}Hg NMR, and single crystal X-ray studies (Table 9) [36–39,42,87–90]. The MeHg(II) cation is the fundamental organomercury species and has been studied as a model spectroscopic probe for binding of metal ions to complex molecules and also finds application as a probe for the study of polynucleotides and proteins [101]. Infrared spectra reveal an uncoordinated NO_3 group [87]. ^1H and ^{13}C NMR studies of complexes of $MeHgNO_3$ with 2,2′-bipyridines and 1,10-phenanthrolines lead to interesting results (Table 17) [36]. Bipyridine and its derivatives form chelates with difficulty with $MeHgNO_3$. This study however, throws light on the chelating ability of the bpy ligands in solution. With the exception of [MeHg(3-dmbpy)](NO_3), the coupling constants, $J(^1H–^{199}Hg)$, for the methylmercury group are similar in complexes of bpy and phen ligands (235.1–239.8 Hz), and are higher than in the 1 : 1 monodentate pyridine complexes (225.2–229.6 Hz). The higher values are assumed to indicate chelation, and consistent with this, the ligand 3-dmbpy, which cannot act as a chelate, forms a complex with a value of $J(^1H–^{199}Hg)$ (230.4 Hz) similar to complexes of unidentate ligands. An sp^2 hybridization scheme for the three-coordinate complexes would alter the *s*-electron density in the mercury–carbon bond to a value lower than that

TABLE 17

^1H and ^{13}C NMR data for ($MeHgNO_3$) complexes [a]

Compound	$\delta^{13}C$(MeHg) [b] (ppm)	δ^1H(MeHg) [c] (ppm)	$J(^1H–^{199}Hg)$ (Hz)
$MeHgNO_3$	−72.5	−2.597	251.8
[MeHg(bpy)](NO_3)	−72.9	−2.499	238.8
[MeHg(6-dmbpy)](NO_3)	−70.2	−2.508	235.9
[MeHg(5-dmbpy)](NO_3)	−73.0	−2.518	237.0
[MeHg(4-dmbpy)](NO_3)	−73.1	−2.550	235.1
[MeHg(3-dmbpy)](NO_3)	−71.6	−2.893	230.4
[MeHg(phen)](NO_3)	−72.8	−2.383	239.8
[MeHg(2-dmp)](NO_3)	−70.3	−2.384	236.0
[MeHg(4-dmp)](NO_3)		−2.416	236.8
[MeHg(5-dmp)](NO_3)		−2.396	238.6

[a] All data from ref. 36.

[b] Chemical shifts w.r.t. internal 1,4-dioxane; accuracy to ca. ±0.1 ppm.

[c] Chemical shifts w.r.t. internal 1,4-dioxane; accuracy to ±0.005 ppm.

found in the linear complexes and thus lower $J(^1H-^{199}Hg)$ [61a,b,104]. However, as seen above, the $J(^1H-^{199}Hg)$ values for three-coordinate complexes are somewhat higher, and this small increase indicates only a slight alteration in *s*-electron density of the hybrid orbital of mercury bonding to carbon and/or a slight alteration of effective charge on the mercury and carbon atoms with consequent contraction or expansion of the valence *s* orbitals. Small upfield shifts of the ^{13}C resonances of the methylmercury group upon increase in coordination number are assumed to indicate only minor changes in effective charge on mercury and carbon. The mercury–carbon coupling constant, $J(^{13}C-^{199}Hg)$, for the complexes is expected to be more sensitive than $J(^1H-^{199}Hg)$ to changes in mercury–carbon bonding, but such data are not reported. Since NMR data indicate only slight changes in mercury–carbon bonding upon increase in the coordination number of mercury, it is apparent that mercury–carbon bonding is the dominant bonding requirement, and hence an *sp*-hybridization scheme similar to that in complexes of the pyridine ligands may be a suitable bonding model for three-coordinate complexes.

The crystals of $[MeHg(bpy)](NO_3)$ are triclinic with space group $P\bar{1}$ (Table 3) [36,37,89]. The mercury has three-coordinate planar geometry with an unsymmetrically chelated bpy ligand (C–Hg–N angle, 164.0°) (Figs. 9 and 10). In other words, the Hg–N bond (2.24 Å) is stronger than Hg–N′ (2.43 Å), and both are longer than the Hg–N distance (2.12 Å) in linear

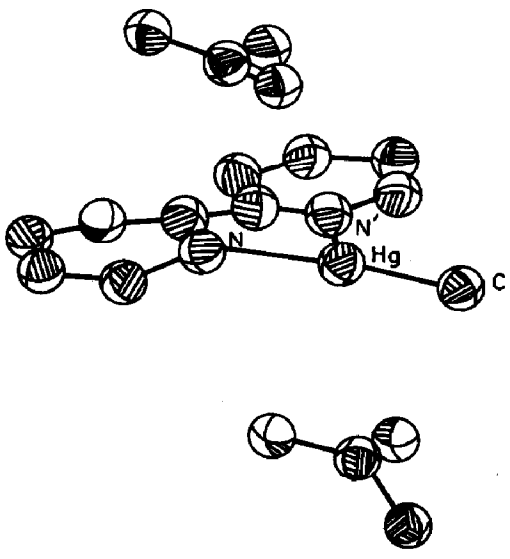

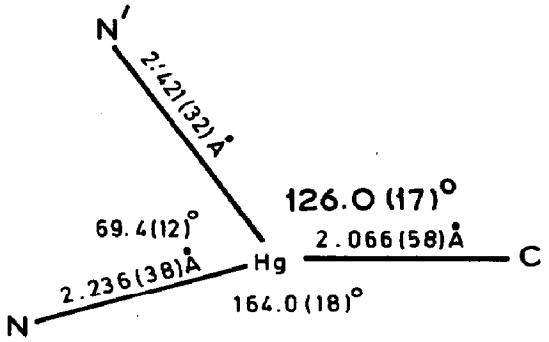

Fig. 9. Structure of $[MeHg(bpy)](NO_3)$ showing the positions of neighbouring NO_3 ions. (Reproduced with permission from J. Organomet. Chem., 88 (1975) C31.)

Fig. 10. Stereochemistry of mercury in the $[MeHg(bpy)]^+$ ion. (Reproduced with permission from J. Organomet. Chem., 88 (1975) C31.)

$[MeHg(py)]^+$ [43]. These distances are similar to those found in phen and bpy complexes of mercury(II) halides or pseudo halides [102,103]. The distortion from trigonal geometry reflects the strong tendency for linear two coordination in organomercury compounds [43,104]. There are two nitrate oxygen atoms at distances of 2.990 and 2.993 Å from mercury(II), one above and one below the $[MeHg(bpy)]^+$ group.

The adduct $[MeHg(3\text{-}dmbpy)](NO_3)$ is monoclinic with space group $P2_1/c$ (Table 3) [38]. The adduct has a bent C(1)–Hg–N(1) group (172.7°) with Hg–C(1) and Hg–N(1) distances of 2.01 and 2.11 Å, respectively. There is weak interaction between the Hg and nitrate oxygen atoms and weak intramolecular π-interaction between Hg and the second pyridyl ring, with Hg–C(2′) 3.11(1), Hg–N(1′), 3.29(1) Å and an angle of 100.5° between the planes of the pyridyl rings (Fig. 11).

The adducts $[MeHgL](NO_3)$ (L = terpy, Et_3terpy, py_2CH_2, py_2CMe_2, py_2CEt_2 and py_3CH) have been studied by ^1H NMR spectroscopy in the solution phase and X-ray crystallography in the solid state (Table 9) [42,90]. The spin–spin coupling constants, $^2J(^1H-^{199}Hg)$, of terpy and Et_3terpy adducts are well removed from those for unidentate pyridines, hence these ligands are not acting as unidentates via the outer pyridine rings, which are expected to be more basic than the central ring (Table 18). The protons of MeHg(II) are 0.31–0.44 ppm upfield relative to the 2,2′-bipyridyl complexes, indicating that at least one pyridyl ring is uncoordinated. Consequently, both terpy and Et_3terpy are acting as bidentates in methanol with one outer ring uncoordinated.

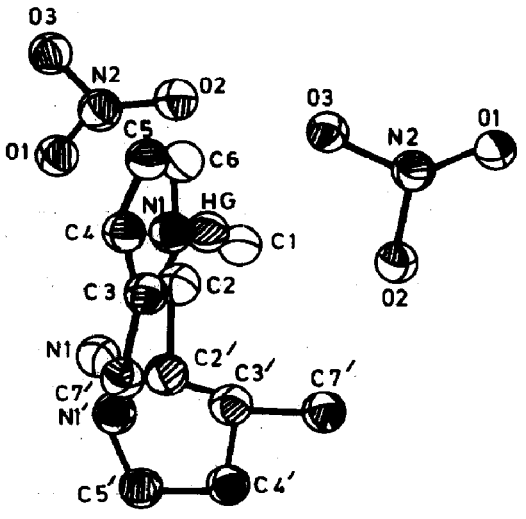

Fig. 11. A stereoscopic view of the structure of $[MeHg(3\text{-}dmbpy)](NO_3)$ showing the relationship between Hg and the nearest NO_3 ion. (Reproduced with permission from Acta Crystallogr., Sect. B, 34 (1978) 3229.)

Somewhat higher values of $J(^1H-^{199}Hg)$ than observed for the 2,2′-bipyridyl complexes reflect the presence of different geometry and binding by nitrogen donors of terpyridyls of differing basicity. The adducts of py_2CH_2 and py_2CR_2 (R = Me, Et) have $J(^1H-^{199}Hg)$ values higher than the unidentate pyridines, suggesting bidentate behaviour. Further, consistent with bidentate behaviour for py_2CH_2, the MeHg(II) proton absorption is not shifted upfield from values for unidentate pyridines. However, the complexes of py_2CR_2 have proton resonances 0.17–0.46 ppm upfield from the pyridine complexes and thus these ligands are unidentate. The upfield shift of the MeHg(II) protons occurs if one potential donor ring of the ligand is shielding that proton by ring current anisotropy. For example, for the 3-dmbpy complex (unidentate), the MeHg(II) proton resonance is 0.2–0.4 ppm upfield of the other pyridine and 2,2′-bipyridyl complexes. The unidentate behaviour of py_2CR_2 may result from the steric constraint of the alkyl substituents, and the steric effect of the CR_2 group in the α-position of the coordinated ring may affect the C–Hg–N bonding geometry and hence $J(^1H-^{199}Hg)$. The value of $J(^1H-^{199}Hg)$ for the complex $[MeHg(py_3CH)](NO_3)$ is higher than for the pyridine, py_2CH_2 and py_2CR_2 complexes, and the MeHg(II) proton resonance is not shifted upfield from values for unidentate pyridines, which is consistent with the presence of py_3CH as a tridentate ligand. However, although py_3CH is clearly not present as a unidentate ligand, molecular models indicate that for bidentate behaviour the uncoordinated pyridyl ring is not constrained to be in an orientation which will shield the MeHg(II) protons, although such an orientation is possible. Thus the ^1H NMR method does not allow assignment of the structure of this complex.

TABLE 18

^1H NMR data of $[MeHgL](NO_3)$ adducts (L = terpy, etc.) [a]

Complex	δ(MeHg) [b,c] (ppm)	$\lvert J(^1H-^{199}Hg)\rvert$ [d] (Hz)
$[MeHg(terpy)](NO_3)$	−2.86	243.0
$[MeHg(Et_3terpy)](NO_3)$	−2.94	243.1
$[MeHg(py_2CH_2)](NO_3)$	−2.49	235.4
$[MeHg(py_2CMe_2)](NO_3)$	−2.85	234.7
$[MeHg(py_2CEt_2)](NO_3)$	−2.93	232.5
$[MeHg(py_3CH)](NO_3)$	−2.43	243.1

[a] All data from ref. 42.
[b] Solution ca. 0.1 M in CD_3OD.
[c] δ values w.r.t. internal standard 1,4-dioxane.
[d] Sign of the coupling constant assumed to be negative [42a,b].

The crystalline complex $[MeHg(py_2CH_2)](NO_3)$ with space group $P2_1/n$ has a distorted T-shaped coordination geometry based on a dominant C–Hg–N moiety (C–Hg–N 172°(1)) (Table 3) [42]. The moiety $CHgN_2$ is approximately planar with a Hg–N distance of 2.16(1) Å (stronger) and a Hg–N′ distance of 2.75(2) Å (weaker). The crystalline $[MeHg(Et_3terpy)]$

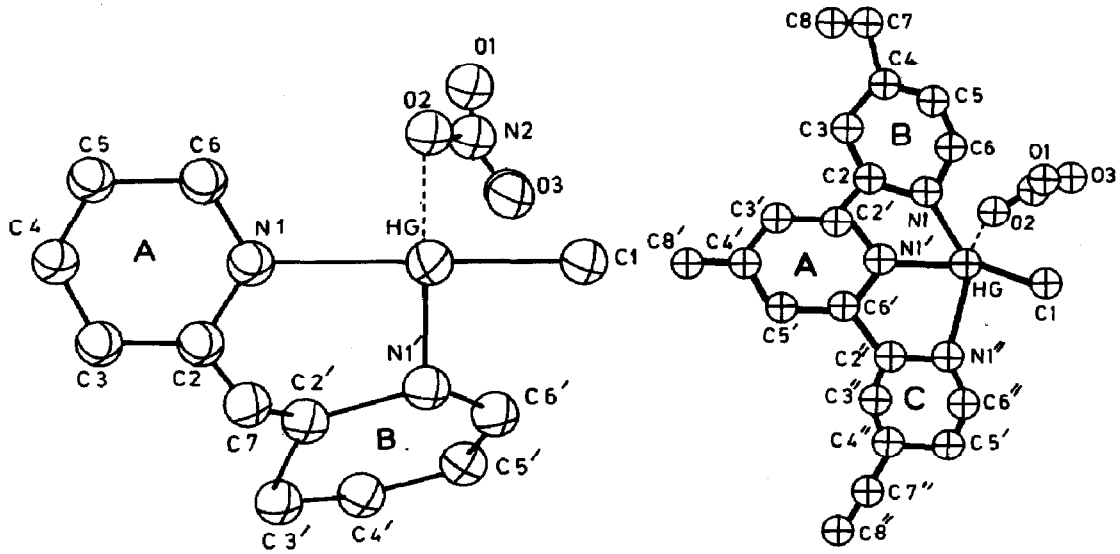

Fig. 12. Structure of the cation $[MeHg(py_2CH_2)]^+$ showing the relationship between Hg and the nearest NO_3 ion. (Reprinted with permission from Inorg. Chem., 20 (1981) 2414.)

Fig. 13. Structure of the cation $[MeHg(Et_3terpy)]^+$ showing the relationship between Hg and the nearest NO_3 ion. (Reproduced with permission from Inorg. Chem., 20 (1981) 2414.)

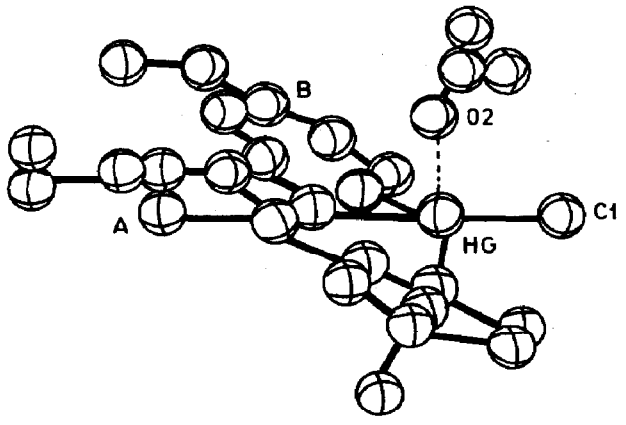

Fig. 14. Structure of $[MeHg(Et_3terpy)]^+$ showing the angles between the pyridyl ring and planes of Et_3terpy. (Reproduced with permission from Inorg. Chem., 20 (1981) 2414.)

(NO_3) has space group $P2_1/n$ and the tridentate ligand is strongly bonded to the central nitrogen [2.26(2) Å, C–Hg–N, 171(1)°] and weakly bonded to the terminal nitrogens [2.51(2) and 2.61(2) Å]. This complex has a highly distorted square planar structure. In both complexes, there is one weak Hg · · · O(2) interaction [2.65(2) Å, L = py_2CH_2; 2.78(2) Å, L = Et_3terpy] (Figs. 12–14).

(iii) Adducts of mercury(II) cyanide

Adducts of mercury(II) cyanide are shown in Table 19. Mercury(II) cyanide is a relatively strong Lewis acid.

The adducts $Hg(CN)_2L$ (L = bpy, phen, 2-dmp, en, thiourea, etc.) have been studied mainly by IR spectroscopy. Thiourea coordinates to Hg via its sulphur donor for well known reasons [39,105–111]. In all of these complexes the CN group remains covalently bound. The bpy, phen and 2-dmp ligands show their usual behaviour. The ligands 4-bpy and its dioxide form polymeric tetrahedral complexes via bridging through the ligands rather than the CN group. The polymerization is attributed to the stereochemical re-

TABLE 19

Adducts of mercury(II) cyanide with various ligands

Compound	Ligand (L)	Techniques used	Refs.
1. (a) $Hg(CN)_2L$	phen, bpy, 2-dmp, en, 3-pn, bn, 5-pn	IR and molar conductance	105–107
(b) $Hg(CN)_2L$	3-pn, en, tren	IR solution phase study	108–110
(c) $Hg(CN)_2L_2$	H_2NCSNH_2	IR solution phase study	108–110
(d) PhHg(CN)L	phen	IR and X-ray	39
(e) $Hg(CN)_2L$	4-bpy, 4-bpyo$_2$	IR	111
2. (a) $Hg(CN)_2L_2$	Me_3P, Ph_3P, *p*-Tol_3P, Cy_3P	IR, Raman, mol. wt. conductance and ^{31}P NMR	105, 112–114
(b) $Hg(CN)_2L$	(i) Cy_3P, t-Bu_3P	IR, Raman, mol. wt., conductance and ^{31}P NMR	105, 112–114
	(ii) Ph_3P	X-ray	40
(c) $Hg(CN)_2L$	*cis*-($Ph_2PCH{=}CHPPh_2$)	^{31}P NMR	40
(d) $Hg(CN)_2L$	dmdp, dmda, opda	IR	115
3. $[C(NO_2)_3]_2HgL$	Ph_3PO, Me_2SO	IR	116
4. (a) $Hg(CN)_2L_n$	n-Bu_3P, Cy_3P $n = 1,2$	solution phase ^{31}P and ^{199}Hg NMR study (CH_2Cl_2 solvent)	117
(b) $Hg(CN)_2L$	n-Bu_3P	solution phase ^{31}P and ^{199}Hg NMR study (CH_3OH solvent)	117

quirements of the ligands [78]. No X-ray study has been reported for any one of the above adducts.

The adduct (PhHgCN)·phen is monoclinic with space group $P2_1/a$ [39]. The mercury atom is four-coordinate. The three rings of the phen ligand are in the same plane, forming an angle of 89° with the plane of the phenyl group. The geometry about Hg is irregular, with different bond angles [C(1)–Hg–C(19), 167.5°; C(19)–Hg–N(1), 93.1°; N(1)–Hg–N(2), 61.8°; and N(2)–Hg–C(1), 95.4°] (Fig. 15).

The ligands Me_3P, Ph_3P, Cy_3P and p-Tol_3P form 1 : 2 (metal : ligand) adducts, whereas dmdp, dmda, opda and *cis*-$Ph_2PCH{=}CHPPh_2$, as well as the bulky ligands Cy_3P and t-Bu_3P, form 1 : 1 adducts [43,105,112–115]. The adducts $(p\text{-}Tol_3P)_2Hg(CN)_2$ and $(Cy_3P)_2Hg(CN)_2$ exist as monomers in CH_2Cl_2, but the adduct $(Ph_3P)_2Hg(CN)_2$ shows significant dissociation (mol. wt. calc. 776, found 555). The adduct $Cy_3PHg(CN)_2$ exists as a dimer in benzene (calc. 523, found 1000). The adducts $Cy_3PHg(CN)_2$ (mol. wt. calc. 532, found 644) and t-$Bu_3PHg(CN)_2$ (mol. wt. calc. 454, found 618) in CH_2Cl_2 indicate partial dissociation of the dimeric species into monomers.

The Raman spectrum of solid $(p\text{-}Tol_3P)_2Hg(CN)_2$ shows a strong band at 2146 cm^{-1} and a weak band at 2141 cm^{-1} in the C≡N stretching region. The complex $(Cy_3P)_2Hg(CN)_2$ shows two Raman bands at 2143 cm^{-1} (strong) and 2130 cm^{-1} (weak). A very strong broad band at 2140 cm^{-1} was observed for $(Ph_3P)_2Hg(CN)_2$. The absorption due to ν(CN) in the IR spectra was very weak for all three adducts. The adduct $(p\text{-}Tol_3P)_2Hg(CN)_2$ shows two weak IR bands at 2145 and 2130 cm^{-1}, unlike the adducts of

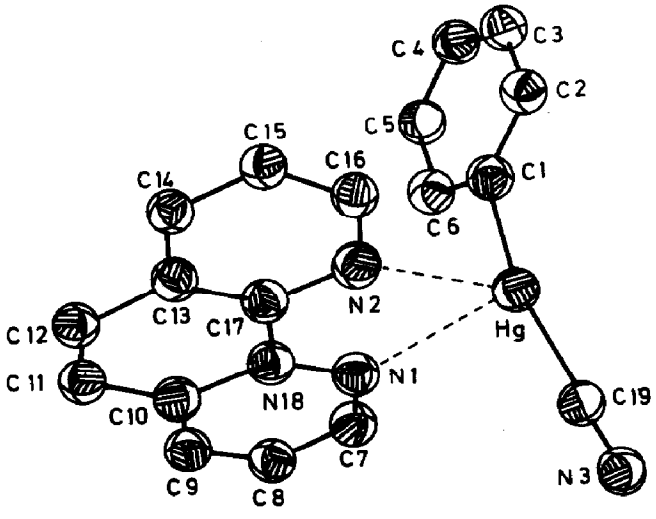

Fig. 15. ORTEP drawing of (PhHgCN)phen. (Reproduced with permission from Acta Crystallogr., 34B (1978) 2711.)

Ph_3P and Cy_3P which show one band each at ca. 2140 cm^{-1} [118]. Molecular weight, IR and Raman spectral data (IR 2146w, 2180w cm^{-1}; Raman 2149s, 2179w cm^{-1}) of $(Cy_3P)Hg(CN)_2$ suggest a centrosymmetric dimeric structure of C_{2v} symmetry. The higher frequency CN bands are attributed to CN bridging [119,120]. The adduct $(t\text{-}Bu_3P)Hg(CN)_2$ shows one strong Raman band at 2152 cm^{-1} and a medium IR band at 2152 cm^{-1}. Although definitive structure conclusions for the 1 : 1 adducts must await X-ray diffraction studies, molecular weight and vibrational spectral data for $(Cy_3P)Hg(CN)_2$ are consistent with a dimeric structure with each mercury atom tetrahedrally coordinated. The 1 : 1 $t\text{-}Bu_3P$ adduct appears to have a similar structure.

In the ^{31}P NMR spectra of some adducts, phosphine single peaks at ambient temperature were observed for the less basic and less bulky phosphines, e.g. Ph_3P and $p\text{-}Tol_3P$, whereas Cy_3P and $t\text{-}Bu_3P$ show a main peak with two satellite peaks due to $J(^{31}P\text{–}^{199}Hg)$ coupling (Table 20). Similar satellites were observed for $(Ph_3P)_2Hg(CN)_2$ and $(p\text{-}Tol_3P)_2Hg(CN)_2$ at low temperature (183 K). The ^{31}P NMR spectra of the Ph_3P and $p\text{-}Tol_3P$ adducts containing excess phosphine gave a single resonance peak even at 183 K, showing that the rate of phosphine exchange is increased markedly by the added phosphine. The ^{31}P NMR spectrum of an equimolar mixture of $(Cy_3P)Hg(CN)_2$ and Cy_3P at ambient temperature was identical to that of $(Cy_3P)_2Hg(CN)_2$. The addition of one more equivalent of Cy_3P, however, gave a spectrum showing only a single resonance peak. Upon cooling the solution to 183 K, the spectrum showed characteristic peaks of the 1 : 2 complex and free phosphine. It is concluded that phosphine exchange occurs

TABLE 20

^{31}P NMR data for some $Hg(CN)_2$ adducts

Compound	δ (ppm)		$\Delta\delta$ (ppm) [a,b]		$J(^{31}P\text{–}^{199}Hg)$ (Hz)		Refs.
	Ambient temp.	183 K	Ambient temp.	183 K	Ambient temp.	183 K	
$(Ph_3P)_2Hg(CN)_2$	12.6	18.7	18.4	22.7		2645	114
$(p\text{-}Tol_3P)_2Hg(CN)_2$	5.0	16.2	13.5	28.2		2766	114
$(Cy_3P)_2Hg(CN)_2$	36.5	37.3	27.6	29.1	3416	3544	114
$(Cy_3P)Hg(CN)_2$	50.4	50.4	41.8	42.2	4560	4998	114
$(t\text{-}Bu_3P)Hg(CN)_2$	87.0	82.6	26.3	21.6	4604	4858	114
	$\delta(^{31}P)$ (ppm)		$J(^{199}Hg\text{–}^{31}P)$ (Hz)				
$Hg(CN)_2(Ph_2PCH{=}CHPPh_2)$		7.2			1525		40

[a] Spectra recorded in CH_2Cl_2; δ are downfield relative to external reference, 85% H_3PO_4.
[b] δ(complex) − δ(phosphine).

via an associative mechanism. There is an increase in the values of $J(^{31}P-^{199}Hg)$ with a decrease in temperature. Similar behaviour is observed for mercury(II) halide and carboxylate adducts [121,122]. The increase in the latter case has been attributed to a decrease in the rate of phosphine exchange with decreasing temperature. Nevertheless, further investigations are needed to explain the temperature-dependence of the spin–spin coupling.

The complex $Hg(CN)_2(PPh_3)_2$ with space group $Pn2_1/a$ (Table 3) has a structure between a tetrahedron and a trigonal pyramid [40]. The Hg–P bonds are different; the short P(1)–Hg bond bends towards, and the long P(2)–Hg bond bends away, from the C(1)HgC(2) plane. Consequently, the angles P(1)HgC(1) and P(1)HgC(2) (116.7 and 114.7°, respectively) are larger than the angles P(2)HgC(1) and P(2)HgC(2) (103.8 and 103.6°, respectively). The angles P(1)HgP(2) and C(1)HgC(2) are 108.9 and 107.8°, respectively (Fig. 16).

Other 1 : 2 adducts probably have structures similar to that of Ph_3P. The adduct of opda has been assigned a chelated tetrahedral stereochemistry based on IR spectra [115]. The complexes with dmdp and dmda require further investigation for establishing the chelating or bridging nature of the ligands. The complex with *cis*-$Ph_2PCH{=}CHPPh_2$ presumably has a chelated tetrahedral structure supported from X-ray and other studies of an analogous complex, $HgBr_2$(*cis*-$Ph_2PCH{=}CHPPh_2$) [40]. The adducts of bis(trinitromethyl)mercury(II) with Ph_3PO and Me_2SO are stable, possibly due to the greater electronegativity of trinitromethyl and hence the greater Lewis acidity of the organomercurial.

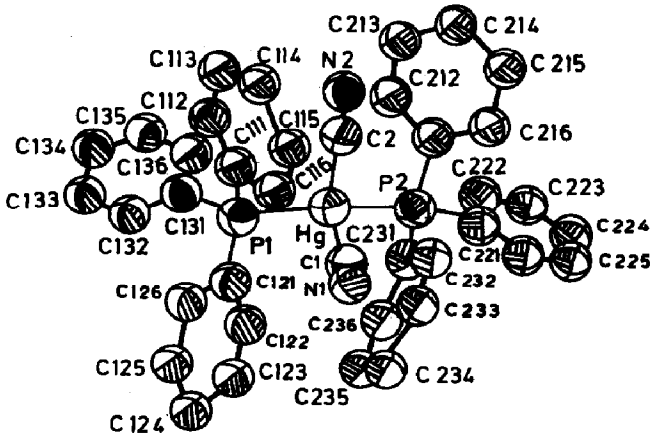

Fig. 16. Molecular structure of the complex $Hg(CN)_2(PPh_3)_2$. (Reproduced with permission from Inorg. Chem., 21 (1982) 1246.)

(iv) Applications of ^{199}Hg NMR to organomercury(II) and mercury(II) adducts

In recent years it has been noted that ^{199}Hg NMR spectroscopy is becoming very useful for studying the coordination chemistry of mercury(II). This is because ^{199}Hg NMR shifts are very sensitive to the immediate environment of the mercury atom [123a–c]. However, the ^{199}Hg NMR data available are limited, but there is still enough to demonstrate the potential of the technique for determining the coordination number of mercury. This section deals with ^{199}Hg NMR data, not only of organomercury(II), but other mercury(II) systems, so as to provide sufficient useful comparative information.

Canty et al. [88] have employed ^{199}Hg NMR spectroscopy for the study of the adducts [MeHgL](NO$_3$) (L = bpy, 3-dmbpy, 4-dmbpy, 5-dmbpy, 6-dmbpy and phen). There is an upfield shift relative to MeHgNO$_3$ indicating increased shielding on coordination by the ligands (Table 21). The spin–spin coupling constant and chemical shift values, $\delta(^{199}Hg)$, favour chelation by the ligands, with the exception of 3-dmbpy. In the ^{1}H NMR method, the increase in coupling constant $J(^1H–^{199}Hg)$ takes place with increase in electronegativity of X in the MeHgX compounds [123,124]. An increase in

TABLE 21

NMR parameters for the MeHg group in [MeHgL](NO$_3$) complexes, together with pK_a values of LH$^+$ [a]

Complex	$\delta(^{199}Hg)$ [b]	$\lvert J(^1H–^{199}Hg)\rvert$ [c]	pK_a of LH$^+$
MeHgNO$_3$		251.8	
[MeHgpy]NO$_3$	−87.0	229.6	4.09
[MeHg(2-mpy)]NO$_3$	−132	227.9	4.71
[MeHg(3-mpy)]NO$_3$	−91	228.2	4.49
[MeHg(4-mpy)]NO$_3$	−98	227.5	4.72
[MeHg(2,4-dmpy)]NO$_3$	−148	225.7	5.44
[MeHg(2,6-dmpy)]NO$_3$	−171	225.2	5.28
[MeHg(2-bzpy)]NO$_3$	−165	229.6	3.97
[MeHg(bpy)]NO$_3$	−236	238.8	3.18
[MeHg(6-dmbpy)]NO$_3$·H$_2$O	−255	235.9	3.99
[MeHg(5-dmbpy)]NO$_3$	−229	237.0	3.76
[MeHg(4-dmbpy)]NO$_3$	−278	235.1	3.97
[MeHg(3-dmbpy)]NO$_3$	−187	230.4	3.59
[MeHg(phen)](NO$_3$)	−351	239.8	4.03

[a] All data from ref. 88.

[b] ca. 0.1 M solutions in CH$_3$OH. Shifts are ppm upfield from MeHgNO$_3$. Accuracy to ±2 ppm.

[c] 0.1 M solutions in CD$_3$OD at 100 MHz. Accuracy to ±0.5 Hz. The sign of coupling constant assumed to be negative.

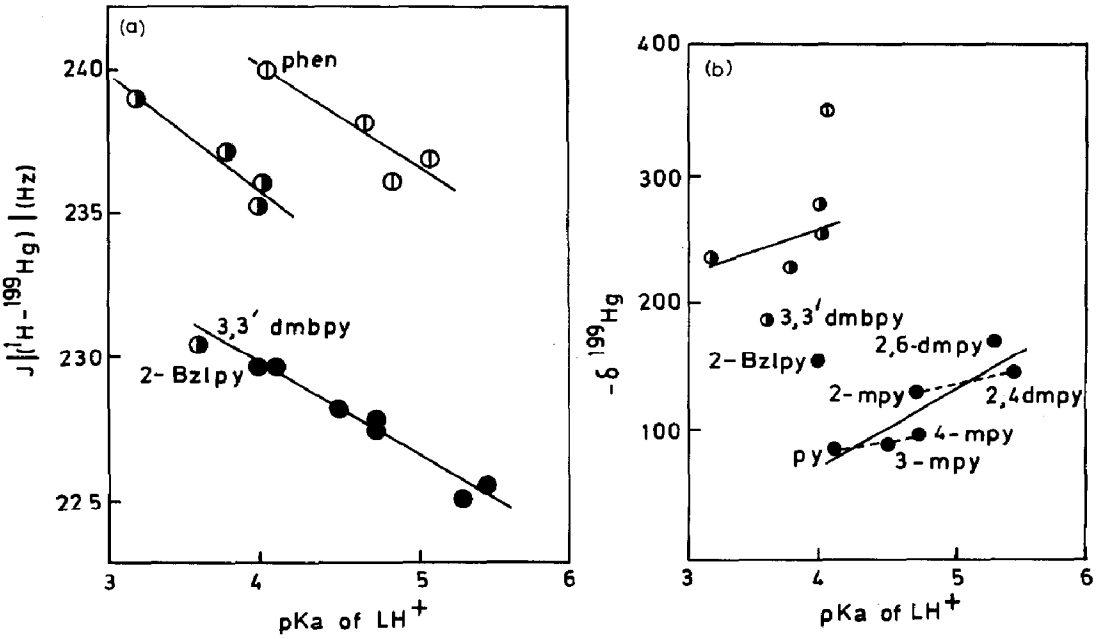

Fig. 17(a). Relationship between $|J(^1H-^{199}Hg)|$ and pK_a of LH^+ in $[MeHgL](NO_3)$ [(L = pyridines (●), 2,2′-bipyridyls (◑) and 1,10-phenanthrolines (Φ)]. Least-squares lines are drawn for each group of ligands with 3,3′-dmbpy excluded. (Reproduced with permission from J. Organomet. Chem., 144 (1978) 371.)

Fig. 17(b). Relationship between $\delta(^{199}Hg)$ and pK_a of LH^+ in $[MeHgL](NO_3)$. (Ligand description of Fig. 17(a).) Least squares lines are drawn for each group of ligands with 3,3′-dmbpy and 2-Bzlpy excluded. (Reproduced with permission from J. Organomet. Chem., 144 (1978) 371.)

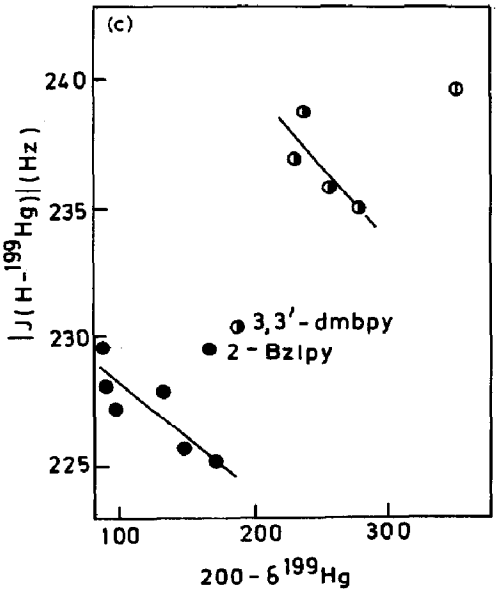

Fig. 17(c). Relationship between $|J(^1H-^{199}Hg)|$ and $\delta(^{199}Hg)$ in the complexes $[MeHgL](NO_3)$. (Ligands description of Fig. 17(a).) Least-square lines are drawn for each group of ligands with 3,3′-dmbpy and 2-Bzlpy excluded. (Reproduced with permission from J. Organomet. Chem., 144 (1978) 371.)

the electronegativity of X is expected to increase the *s*-character of the hybrid orbital of Hg involved in bonding to carbon (Fermi contact term), and to increase the effective nuclear charge for the mercury 6*s* orbital, resulting in contraction of that orbital [123–125]. Thus, for [MeHgL](NO$_3$), $J(^1H-^{199}Hg)$ increases with decreasing pK_a of LH$^+$, with separate relationships for uni- and bi-dentate ligands. A lower basicity of L corresponds to a greater electronegativity of the nitrogen donor atom of L (Table 21, Fig. 17(a)). However, application of the above approach to ^{199}Hg NMR results is not straightforward. Thus plots of $\delta(^{199}Hg)$ versus pK_a of LH$^+$ (Fig. 17(b)) and $J(^1H-^{199}Hg)$ (Fig. 17(c)) give only approximate correlations for the unidentate ligands, with 2-benzylpyridine (2-Bzlpy) and 3-dmbpy well removed from the correlation; correlations for the bidentate ligands are poor.

In Fig. 17(b), the shifts for the linear complexes reflect greater shielding of Hg with the more basic ligands (bold line) and suggest that methyl substitution in the 2-position may also result in an additional upfield shift of ca. 30 ppm, as a separate correlation can be drawn for py, 3-methylpyridine, 4-methylpyridine, 2-methylpyridine and 2,4-dmpy (dotted line). Double substitution, as in 2,6-dmpy, causes a further 30 ppm shift. Two linear complexes, 2-bzpy and 3-dmpy, correlate neither with the other linear complexes nor with chelated ligands, and have values of $\delta(^{199}Hg)$ higher than complexes of unidentate ligands of similar basicity. In addition to a possible effect from substitution in the 2-position, the high values may indicate the presence of a weak interaction between Hg and the aromatic ring [126].

The correlation between $\delta(^{199}Hg)$ and $J(^1H-^{199}Hg)$ for linear complexes is as expected (Fig. 17(c)). Complexes with a greater effective nuclear charge on Hg (i.e. complexes with lower $\delta(^{199}Hg)$ and lower pK_a values of LH$^+$) have higher values of $J(^1H-^{199}Hg)$. The complexes of 2-bzpy and 3-dmbpy are again exceptions, but when $J(^1H-^{199}Hg)$ is plotted against pK_a, these complexes conform with the other linear complexes. This suggests that $J(^1H-^{199}Hg)$ is insensitive to some of the factors determining the ^{199}Hg chemical shift, in particular substitution in the 2-position of pyridine. The bidentate ligands bpy, phen, 4-dmbpy, 5-dmbpy and 6-dmbpy have also been shown by ^{1}H NMR spectroscopy to give three-coordinate mercury. For these complexes, the shifts correlate less well with pK_a, and $J(^1H-^{199}Hg)$ is higher than for linear complexes although the mercury atom is more shielded. As for the complexes of 2-bzpy and 3-dmbpy, $J(^1H-^{199}Hg)$ may be insensitive to some of the factors determining the ^{199}Hg chemical shift.

Another study by Colton and Dakternieks [117] has made intensive investigations into ^{31}P and ^{199}Hg NMR applications to the formation of a series of mercury(II) complexes. $HgA_2(phos)_{1-4}$ [A = ClO_4^-, NO_3^-, CF_3COO^-, CH_3COO^-, SCN^-, CN^-, Cl^-, Br^- and I^-; phos = $(4\text{-}ClC_6H_4)_3P$, $(4\text{-}MeOC_6H_4)_3P$, $(2\text{-}MeOC_6H_4)_3P$, $(4\text{-}CH_3C_6H_4)_3P$, $(2\text{-}CH_3$-

$C_6H_4)_3P$, $(3\text{-}CH_3C_6H_4)_3P$, Bu^n_3P, Cy_3P and Ph_3P] in CH_2Cl_2 solution. The steric effect of the ligands and the nature of the anion, A, influence the number of phosphines coordinated to mercury. ^{31}P and ^{199}Hg NMR data for a series of adducts, $Hg(ClO_4)_2(phos)_n$, are given in Table 22. In each case the ^{31}P NMR spectrum consists of a single line accompanied by Hg satellite. The ^{199}Hg NMR spectrum of each complex consists of a triplet with the Hg–P coupling constant equal to that derived from the ^{31}P NMR spectrum. There is no evidence for the formation of 1 : 1 adducts with $Hg(ClO_4)_2$ in a 1 : 1 stoichiometric mixture of a phosphine and $Hg(ClO_4)_2$. The addition of sterically bulky phosphines, PCy_3, $(2\text{-}CH_3OC_6H_4)_3P$ and $(2\text{-}CH_3C_6H_4)_3P$, to the appropriate $Hg(ClO_4)_2(phos)_2$ solution does not affect the spectra except for the free phosphine ^{31}P spectrum. However, the addition of one equivalent of $P(4\text{-}CH_3C_6H_4)_3$ and $P(3\text{-}CH_3C_6H_4)_3$ to the appropriate $Hg(ClO_4)_2(phos)_2$ solution leads to the quantitative formation of new species, $Hg(ClO_4)_2(phos)_3$. Further addition of phosphine to solutions containing $Hg(ClO_4)_2(phos)_3$ induces phosphine exchange in all cases, but on cooling, sharp resonances with Hg satellites are observed indicating the formation of

TABLE 22

^{31}P and ^{199}Hg NMR data for $Hg(ClO_4)_2(phos)_n$ in CH_2Cl_2 solution [a]

Phosphine	n	$\delta(^{31}P)$ (ppm)	$\delta(^{199}Hg)$ (ppm)	J(Hg–P) (cps)	Temperature (°C)
$P(4\text{-}ClC_6H_4)_3$	2	43.1	90t	5340	−50
	3	40.3	770q	3255	−50
$P(4\text{-}CH_3OC_6H_4)_3$	2	45.5	180t	4800	30
	3	41.1	880q	3040	30
	4	26.8	850A	2070	−30
$P(2\text{-}CH_3OC_6H_4)_3$	2	3.3	190t	4980	30
$P(4\text{-}CH_3C_6H_4)_3$	2	47.2	200t	4940	30
	3	41.1	885q	3080	−30
	4	29.2	840A	2090	−30
$P(2\text{-}CH_3C_6H_4)_3$	2	39.7	230t	4240	30
$P(3\text{-}CH_3C_6H_4)_3$	2	46.1	255t	5060	30
	3	41.1	895q	3090	30
	4	28.7	880A	2070	−20
$P(C_4H_9)_3$	2	49.8	290t	4280	30
	3	30.6	1080q	3050	−70
	4	4.8	1130A	1980	−70
PCy_3	2	78.3	420t	3730	30
PPh_3	2	47.2		5010	−60
	3	42.8	875q	3120	−30
	4	32.2	845A	2090	−60

[a] All data from ref. 117.

a new complex in addition to three-coordinate Hg. When the stoichiometry is 1 : 4 (metal : phos), only a single species, $Hg(ClO_4)_2(phos)_4$, was indicated. However, the addition of $P(4\text{-}ClC_6H_4)_3$ to a solution of its 1 : 3 adduct produces no further change in the Hg coordination and the ^{31}P NMR spectrum shows only the 1 : 3 adduct and free phosphine. The formation of $Hg(ClO_4)_2(phos)_4$ is the ultimate species because further addition of phosphine produced no evidence for new species.

From the data in Table 22, several trends are observed. An increase in the number of phosphines coordinated to the mercury atom leads to a shift in the position of the ^{31}P frequency to lower frequency (i.e. smaller coordination chemical shift), together with a decrease in the value of $J(^{199}Hg-^{31}P)$ and a shift to higher frequency of the ^{199}Hg resonance. The largest changes in position of the ^{199}Hg resonance take place in going from two- to three-coordinate mercury in $Hg(ClO_4)_2(phos)_3$. These changes are due to increased electron density on Hg from the addition of the third phosphine molecule, as well as a contribution from the change in mercury hybridization from *sp* to sp^2. The addition of the fourth phosphine molecule to give the 1 : 4 adduct produces a much larger shift in the ^{31}P resonance to lower frequency, a reasonable reduction in coupling constant, but only a very small change in the chemical shift of mercury. This suggests that the mercury atom undergoes little overall change in total electron density and that the main change is probably that of hybridization from sp^2 to sp^3 about the mercury atom. But in view of the tendency of organomercury to maintain linearity in CHgC or CHgX moieties, the added ligands are overlapping Hg *p* orbitals which are at higher energy. This would lead to an overall smaller increase in total electron density; an observation which agrees with the observed data. Furthermore, the positions of the phosphorus resonances for the 1 : 2 adducts are surprisingly similar for most of the phosphines and bear no obvious relationship to $J(Hg-P)$ or $\delta(Hg^{199})$, or even to the ^{31}P resonance frequency of the uncoordinated phosphine itself. The positions of the mercury resonances in the two series $Hg(ClO_4)_2(phos)_{3\text{ or }4}$ cover a comparatively small range and appear largely independent of the nature of the phosphine, suggesting that the organic substituents on the phosphine are equally capable of distributing the electron density about phosphorus so that the electron density about Hg is the same for each of these adducts.

Unlike mercury(II) perchlorate, $Hg(CF_3COO)_2$ does form 1 : 1 adducts with most of the phosphines. With one exception, all 1 : 1 adducts show a single ^{31}P NMR peak with ^{199}Hg NMR satellites and a doublet in the ^{199}Hg NMR spectrum with coupling constant equal to that derived from the phosphorus spectrum. In the case of $Hg(CF_3COO)_2(PCy_3)$, a triplet and a singlet were observed in the ^{199}Hg NMR spectrum indicating formation of an asymmetric isomer similar to that observed in $HgI_2(PBu_3)_2$ [127]. The

1 : 1 adducts further react with phosphines forming 1 : 2 adducts, $Hg(CF_3COO)_2(phos)_2$ (Table 23). The effect of further addition of phosphines to the solutions of the appropriate 1 : 2 adducts is dependent on the nature of the phosphine. The ligands PCy_3, $P(2\text{-}CH_3C_6H_4)_3$ and $P(2\text{-}CH_3OC_6H_4)_3$ produced no further reaction. The addition of $P(4\text{-}ClC_6H_4)_3$ to its 1 : 2 adduct induced phosphine exchange, but the 1 : 3 adduct could not be detected even up to −75°C. In all other cases, the formation of $Hg(CF_3COO)_2(phos)_3$ was established. Formation of a 1 : 4 adduct does not take place in any of the phosphines studied.

In the phosphine adducts of $Hg(CF_3COO)_2$, the factors influencing NMR parameters are not easily identified. In each case a large decrease in the value of J(Hg–P) takes place from the 1 : 1 to 1 : 2 adducts, accompanied by a shift to higher frequency of the phosphorus resonance. Simultaneously, the Hg resonance frequency shows an upward shift midway between that found for $Hg(ClO_4)_2(phos)_2$ and $Hg(ClO_4)_2(phos)_3$. This evidence strongly supports coordination by CF_3COO^-. The mode of coordination is also different

TABLE 23

^{31}P and ^{199}Hg NMR data for $Hg(CF_3COO)_2(phos)_n$ in CH_2Cl_2 solution[a]

Phosphine	n	$\delta(^{31}P)$ (ppm)	$\delta(^{199}Hg)$ (ppm)	J(Hg–P) (Hz)	Temperature (°C)
$P(4\text{-}ClC_6H_4)_3$	2	36.4	530t	5950	30
$P(2\text{-}CH_3OC_6H_4)_3$	1	−9.7	55d	10440	30
	2	8.2	370t	6265	30
$P(4\text{-}CH_3C_6H_4)_3$	1	32.8	70d	9100	30
	2	36.4	530t	5760	30
	3	33.6	890q	3340	−30
$P(2\text{-}CH_3C_6H_4)_3$	1	12.4	145d	8920	−30
	2	36.3	485t	5570	−30
$P(3\text{-}CH_3C_6H_4)_3$	1	34.8	75d	9050	30
	2	36.8	580t	5730	30
	3	33.4	920q	3300	−20
$P(C_4H_9)_3$	1	32.9		8500	−50
	2	36.8	630t	5290	−60
	3	23.9	985q	3580	−60
$P(C_6H_{11})_3$	1	69.6	641t	4280	−60
	2	65.1	800s		
			600t	4730	30
PPh_3	1	32.2	30d	9130	−50
	2	36.9	525t	5930	−50
	3	35.1	910q	3310	−50
$P(4\text{-}FC_6H_4)_3$	1	31.0	50d	9300	30
	2	36.3	530t	6300	60

[a] All data from ref. 117.

in 1 : 1 and 1 : 2 adducts. Going from the 1 : 2 to the 1 : 3 adduct, there is a small downward shift in the phosphorus resonance with a further decrease in the coupling constant. The Hg resonance moves to higher frequency. The above evidence suggests that the 1 : 3 adducts of $Hg(CF_3COO)_2$ do not contain a simple $Hg(phos)_3^{2+}$ unit, but CF_3COO^- coordinated to Hg.

Among the phosphine adducts of other Hg(II) salts containing various anions, only PBu_3^n and PCy_3 give adducts having sufficient solubility for ^{199}Hg NMR measurements (Table 24). The nature of the adducts varies from 1 : 1 to 1 : 3. The behaviour of the CH_3COO^- group appears to be similar to that of CF_3COO^-, the differences in the NMR data reflecting the different electronegativities of the anions. The nitrate forms 1 : 1 and 1 : 2 adducts

TABLE 24

^{31}P and ^{199}Hg NMR data for the adducts $HgA_2(phos)_n$ in CH_2Cl_2 [a]

Phosphine	A	n	$\delta(^{31}P)$ (ppm)	$\delta(^{199}Hg)$ (ppm)	J(Hg–P) (Hz)	Temperature (°C)
PBu_3^n	NO_3	1	34.9	110d	9230	−50
		2	41.3	405t	5200	−65
		3	26.9	995q	3470	−65
	CH_3COO	1	29.1	200d	8345	−50
		2	30.7	715t	5600	−65
		3	22.3	1100q	3150	−65
	SCN	1	37.5	815d	6130	30
			36.8	695t	4960	
				725s		
		2	29.7	1115t	4330	30
		3	18.3	1265q	3130	−65
	CN	1	16.4	950d	4500	−70
			12.4	1115t	3660	
		2	10.1	1160t	3410	−70
	Cl	3	15.1	1095q	3590	−75
	Br	3	11.9	1095q	3390	−75
	I	3	7.1	1080q	2840	−105
PCy_3	NO_3	1	63.9	15d	6980	30
		2	66.3	435t	4760	30
	CH_3COO	1	61.4	335d	7465	30
		2	53.5	665t	5240	30
	SCN	2	57.6	970t	4295	30
	CN	1	49.9	950d	4830	−65
		2	37.0	1095t	3440	−65
	CN [b]	1	16.4	950d	4500	−50
			13.8	1113t		

[a] All data from ref. 117.

[b] NMR in CH_3OH solution.

with PBu^n_3 and PCy_3, but no further complex formation is noticed in the case of PCy_3. However, PBu^n_3 does form a 1 : 3 adduct. Varying modes of nitrate coordination are implied by the NMR data. Mercury(II) thiocyanate forms 1 : 1 and 1 : 2 adducts with both ligands. The adduct $Hg(SCN)_2PCy_3$, a polymeric substance (via SCN bridging), is too insoluble for NMR studies [128]. The 1 : 2 adduct is monomeric in benzene, involving Hg–SCN bonding [129]. PBu^n_3 also forms a 1 : 3 adduct. The ^{31}P NMR spectrum of $Hg(SCN)_2PBu^n_3$ shows two resonances, each with ^{199}Hg satellites. The ^{199}Hg NMR spectrum shows a triplet, a doublet and a singlet, and the coupling constants from the multiplets correspond to those derived from the phosphorus spectrum. These results show the presence of both symmetric and asymmetric isomers in a dimeric structure, similar to the iodide complex mentioned earlier. The ligand PCy_3 gives 1 : 1 and 1 : 2 adducts with $Hg(CN)_2$, but no 1 : 3 adduct is detected. The spectrum of the 1 : 1 adduct $Hg(CN)_2(PBu^n_3)$ is identical to the corresponding 1 : 1 adduct of $Hg(SCN)_2$. The cyanide ligand does not permit further coordination by the phosphine ligands to Hg (i.e. 1 : 3 or 1 : 4 adducts).

General comments can be drawn from the series $HgA_2(PBu^n_3)_n$ studied for the entire range of anions. The arrangement of anions for $HgA_2(PBu^n_3)_2$ in order of increasing $\delta(^{199}Hg)$ gives the order: ClO_4^-, NO_3^-, CF_3COO^-, SCN^- and CN^-, which is also a reasonable order of increase in the involvement of the anion in coordination to the mercury atom. The remaining anions lie between these extremes and allow one to three phosphines to coordinate. The systematic variation of the phosphine in the series $Hg(ClO_4)_2(phos)_n$ reflects differences in the coordination of the Hg which result from steric and electronic differences of the phosphines themselves since ClO_4^- ion is not coordinated at all to Hg in CH_2Cl_2 solution. Steric effects are apparent for the phosphines PCy_3, $P(2\text{-}CH_3C_6H_4)_3$ and $P(2\text{-}CH_3OC_6H_4)_3$. An electronic effect must be responsible for the inability of $P(4\text{-}ClC_6H_4)_3$ to coordinate more than three molecules to the metal.

From Fig. 18, it is apparent that, with the exception of SCN, $\delta(^{31}P)$ decreases linearly with increasing $\delta(^{199}Hg)$ in the series $HgA_2(PBu^n_3)_2$. The halide series, $HgX_2(PBu^n_3)_2$, however, shows an increase in $\delta(^{31}P)$ with increase in $\delta(^{199}Hg)$. The attempted correlation between coupling constants J(Hg–P) and either $\delta(^{31}P)$ or $\delta(^{199}Hg)$ yielded no obvious success except within the limited area of adducts of HgX_2 [127,130]. There is some disagreement in the literature about the validity of the attempted correlation between J(Hg–P) and $\delta(^{31}P)$ [131]. Much of the disagreement arises because the complexes are in most cases undergoing rapid anion exchange, with several individual species being exchange-averaged for each compound. In the halide complexes, $HgX_2(PBu^n_3)_2$, anion dissociation occurs, and the equilibria exist in solution with each species contributing to the weighted

average spectrum.

$$HgX_2(PBu^n_3)_2 \rightleftharpoons [HgX(PBu^n_3)_2]^+ + X^- \rightleftharpoons [Hg(PBu^n_3)_2]^{2+} + 2X^-$$

The equilibria lie substantially in favour of coordinated halide, leading to a valid correlation between coupling constants and chemical shifts within the halide complexes. Such correlations are understood in terms of the relative contributions of the halide and phosphine to the coordination sphere of the mercury atom [130].

The correlations of NMR data between the halide adducts and those of the other anions are much more difficult, partly because the equilibrium positions in solution may be different, but also because most of the other anions have the potential to act as both mono- and bi-dentate ligands complicating the equilibria in solution for a labile system. For instance, the adduct $Hg(CH_3COO)_2(PBu^n_3)_2$ could have contributions from $Hg(PBu^n_3)^{2+}_2$ and two forms of $[Hg(CH_3COO)(PBu^n_3)_2]^+$ containing mono- and bi-dentate acetate to give three- and four-coordinated Hg, respectively. Similar arguments hold for $Hg(CF_3COO)_2(PBu^n_3)_2$. It is therefore not surprising that there is poor correlation of NMR data between these systems and the halide systems. It seems reasonable to attempt correlation of NMR data only after it is possible to infer solution structures with certainty.

Finally, it may be worth concluding that in all cases the $\delta(^{199}Hg)$ values appear to move to higher frequency as the coordination number increases. Also, in the perchlorate series there is a steady decrease in $\delta(^{31}P)$ in the sequence $Hg(ClO_4)_2(phos)_{2-4}$, with a corresponding decrease in $J(Hg-P)$. This reflects a gradual decrease in the Hg–P bond strength, also supported by the observation that the rate of phosphine exchange increases as the number of phosphines increases. The halide adducts $HgX_2(phos)_{1-3}$ also show similar trends, but all the potentially bidentate anions fail to show this regular variation.

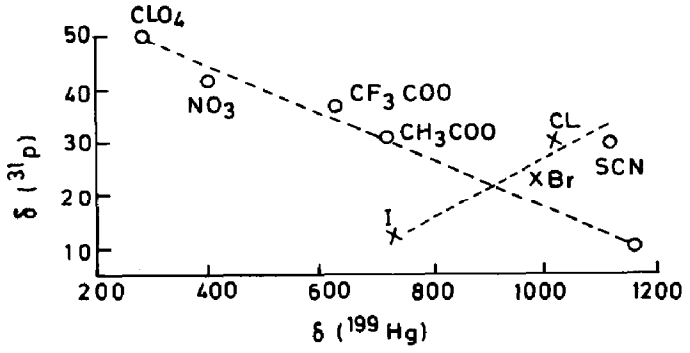

Fig. 18. Plot of $\delta(^{31}P)$ against $\delta(^{100}Hg)$ for a series of complexes $Hg(PBu^n_3)_2A_2$. (Reproduced with permission from Aust. J. Chem., 34 (1981) 323.)

(v) Thermodynamic studies of the adducts

Thermodynamic studies of some of the complexes of organomercury(II) have been reported. These reveal some interesting results about chelation or bridging of a particular ligand.

Thermodynamic data of Hg–ligand interaction involving arylmercury halides ArHgX (Ar = Ph, *o*- and *p*-tolyl, *o*-$MeOC_6H_4$, *p*-$EtOC_6H_4$, *o*- and *p*-chlorophenyl and C_6Cl_5) and bidentate phen and tmed, show that these adducts are more stable than those of monodentate 4-methylpyridine ($K \approx 2$ l mol^{-1}) (Table 25) [132]. However, their enthalpies are only slightly higher, implying the formation of two weak Hg–N bonds. In other words, the higher stability is attributed to chelation of Hg by the ligands. Substitution in the aryl group of ArHgX, even by five chlorine atoms, has little effect on the enthalpy of formation of the adducts with phen. However, the adduct stability is lowered by alkyl or alkoxy substitution and raised by chlorine substitution. The enthalpy of formation of PhHgCl(phen) is greater than that of PhHgBr(phen) by ~ 10 kJ mol^{-1}. However, the bromide adduct is more stable than the chloride adduct. The same is true for the tmed ligand adduct. This suggests that the larger bromine atom has an important entropy effect, perhaps by cooperating with the added base to displace additional solvent molecules.

TABLE 25

Thermodynamic data for 1:1 adducts of ArHgX with phen and tmed (solvent benzene at 30°C) [a]

Ar	X	Ligand	K(l mol^{-1})	$-\Delta H^0$ (kJ mol^{-1})
Ph	Br	phen	798	20.2
Ph	Br	tmed	211	26.3
Ph	Cl	phen	346	30.6
Ph	Cl	tmed	137	33.2
o-$CH_3C_6H_4$	Cl	phen	221	29.2
p-$CH_3C_6H_4$	Cl	phen	298	23.7
p-$CH_3C_6H_4$	Cl	tmed	71	37
o-$MeOC_6H_4$	Cl	phen	193	23.2
p-$C_2H_5OC_6H_4$	Cl	phen	233	26.1
o-ClC_6H_4	Cl	phen	967	29.6
p-ClC_6H_4	Cl	phen	719	26.7
p-ClC_6H_4	Cl	tmed	170	39.9
p-ClC_6H_4	Br	tmed	228	31.5
C_6Cl_5	Cl	phen	> 8000	28.4
C_6Cl_5	Cl	tmed	670	44.8

[a] All data from ref. 132.

When the R group of RHgX is Me, Et, Pr, Bu, $PhCH_2$ or Cy and X = Cl or Br, the thermodynamic data for the interaction of RHgX with phen and tmed show that the stability of the adducts is lower than when R is an aryl group (Tables 25 and 26) [132,133]. This behaviour is in general agreement with the low stability of RHgX complexes when R is an alkyl group.

The stability of the adducts of the chloro derivatives $(Cl_3C)HgCl$ and $(Cl_3C)_2Hg$ with phen and tmed is higher than that of the alkylmercury derivatives (Table 27) [133]. Tri-n-butylphosphine forms dimeric adducts

TABLE 26

Thermodynamic data for 1:1 adducts of RHgX with phen and tmed (solvent benzene at 30°C) [a]

R	X	Ligand	K (l mol^{-1})	$-\Delta H^0$ (kJ mol^{-1})
Me	Br	phen	15.4	26.8
Et	Br	phen	25.1	17.3
Pr	Br	phen	12.6	27.5
Bu^n	Br	phen	18.0	22.2
Cy	Br	phen	27.3	21.0
$C_6H_5CH_2$	Cl	phen	103.1	27.1
Me	Br	tmed	28.2	34.2
Et	Br	tmed	10.8	31.5
Pr	Br	tmed	11.4	28.2
Bu^n	Br	tmed	11.6	34.0
Cy	Br	tmed	2.4	38.3
$C_6H_5CH_2$	Cl	tmed	39.1	40.9

[a] All data from ref. 133.

TABLE 27

Thermodynamic data for 1:1 adduct formation between $(Cl_3C)HgCl$ and $(Cl_3C)_2Hg$ with bpy, phen, tmed and C_4H_8S (benzene solvent at 30°C) [a]

Substrate	Ligand	M (l mol^{-1})	$-\Delta H^0$ (kJ mol^{-1})
$(Cl_3C)_2Hg$	bpy	449	31.4
	phen	$>10^4$	42.3
	tmed	73.3	49.6
	C_4H_8S	7.5	25.3
$(Cl_3C)HgCl$	bpy	326	31.6
	phen	$>10^4$	47.7
	C_4H_8S	10.7	33.3

[a] All data from ref. 133.

$(RHgX \cdot PBu^n_3)_2$ (R = Me, Et, Pr, Bu^n, Cy_3, $C_6H_5CH_2$ and *o*-chlorobenzyl; X = Cl, Br) which have a higher stability, with enthalpies of formation of -60 kJ (g.at.Hg)$^{-1}$ (Table 28) [133]. The Lewis acidity of the compounds increases in the order:

$$R_2Hg \ll RHgCl < (Cl_3C)_2Hg < (Cl_3C)HgCl < HgCl_2$$

Adduct formation between $(Cl_2C{=}CCl)_2Hg$ and bpy, phen, 2-dmp, 3-tmp or dmdp shows that this substrate is a weaker acceptor than $(C_6F_5)_2Hg$ and bis$(C(NO_2)_3)_2Hg$, but stronger than Ph_2Hg [32]. This study clearly demonstrates a unique role of the halogens present in the organic moiety of organomercury(II) adducts in determining the stability of the adducts. A more electronegative substituent usually imparts higher stability. The thermal stability as a function of the ligand increases in the order bpy < phen < 2-dmp < 3-tmp.

Thermodynamic data for adduct formation between $Hg(CN)_2$ and bpy, phen, tmed, etc. indicate that the adducts are much more stable than monodentate nitrogen donors (Table 29) [134,135]. The adduct with the phen ligand is particularly more stable than that with bpy. This may be attributed to the chelate effect indicating four-coordinate mercury [32]. The relative stabilities have been ascribed to the tendency of organomercurials to preserve approximate linearity upon coordination thus necessitating the approaching ligands to interact with *p* orbitals on mercury. Interestingly, there is a decrease in the enthalpy of adduct formation with bpy and phen compared with other ligands. This may be attributed either to weakening of the Hg–N bonds because the misfitting of the bidentate base with the large mercury atom or to an opposing enthalpy change arising from the bending of the linear NC–Hg–CN molecule [136]. Open chain bases having two

TABLE 28

Thermodynamic data for the formation of $(RHgX \cdot PBu^n_3)_2$ (benzene solvent at 30°C) [a]

R	X	$K' \times 10^{-3}$ [b]	$-\Delta H^0$ kJ(g.at.Hg)$^{-1}$)
Me	Br	7.1	65.0
Et	Br	3.2	52.3
Pr	Br	3.3	57.5
Bu	Br	3.6	54.7
Cy	Br	2.6	48.0
$C_6H_5CH_2$	Cl	37.5	64.0
o-$ClC_6H_4CH_2$	Cl	54.0	67.8

[a] All data from ref. 133.
[b] K' in $l^{1.5}$ mol$^{-1.5}$.

TABLE 29

Thermodynamic data for the formation of 1:1 adducts of nitrogen bases with $Hg(CN)_2$ [a]

Ligand [b]	K	$-\Delta H^0$
bpy	175	19.7
phen	$>10^4$	28.6
dmed	$>10^4$	55.5
tmed	$>10^4$	50.8
tmpd	3900	38.7
tmbd	134	30.4

[a] All data from ref. 135.

[b] dmed = *N,N'*-dimethyl-1,2-diaminoethane; tmpd = *N,N,N',N'*-tetramethyl-1,3-diaminopropane; tmbd = *N,N,N',N'*-tetramethyl-1,4-diaminobutane.

nitrogen donors, such as dmed, tmed, tmpd and tmbd, also supply evidence for the effect of chelate ring size on adduct stability (Table 29). The amines with $N-C_2-N$ chains give 1:1 adducts of very high stability, indicating that they are chelates with four-coordinate mercury; the increased enthalpies of formation also support this. These larger enthalpies of reaction also show that there is little loss of enthalpy associated with the mercury atom becoming four-coordinate so that unusually low enthalpies of formation of adducts with bpy and phen must derive from specific or misfitting of these bases with the larger mercury atom and not simply from the bending of the NC–Hg–CN unit. An increase in the chelate ring size to six by using a $N-C_3-N$ chain leads to a distinct reduction in both the enthalpy of adduct formation and adduct stability. The data for the formation of the adduct with tmbd, which would give a seven-membered chelate ring, suggest that either this base is unidentate or the formation of a seven-membered ring adds little to the adduct stability. It has been established that with most nitrogen bases, the enthalpies of adduct formation and adduct stabilities both increase in the order:

$$RHgX \ll Hg(C_6F_5)_2 < Hg(CN)_2 < Hg(CCl_3)_2 < HgX_2 \qquad (X = Cl, Br, I)$$

D. NATURE OF THE BONDING

The energy separation between mercury valence *s* and *p* orbitals is higher than that of zinc and cadmium and hence mercury readily forms linear HgX_2 compounds involving *sp* hybridization. Mercury(II) reacts with a variety of donor atoms, such as O, N, S, P, etc. forming three- and four-coordinate complexes. However, there appears to be no clear cut model for explaining the nature of bonding in these complexes, particularly when

the energy separation between the *s* and *p* orbitals is high. To invoke sp^2 or sp^3 hybridization for three- and four-coordinate complexes may be an oversimplification of the problem. This survey of the literature of organomercury(II) provides some interesting observations on the nature of the bonding involved.

(a) The bonding in PhHg(meoxine) and PhHg(oxine) has been explained as follows (Fig. 8): the arrangement in structure 3 is consistent with the use of mercury *sp* hybrids to bond carbon and oxygen (C–Hg–O, nearly linear, 175°) and a *p* orbital for attachment of nitrogen (more weakly bonded, Hg–N = 2.57 Å > Hg–O = 2.06 Å). The bonding in structure 1 could involve the use of mercury sp^2 hybrids, but *sp* hybridization is also possible with both nitrogen and oxygen interacting with a single *sp* hybrid (O–Hg–N, 73°) [74]. The latter description is preferred since the use of the hybridization (*sp*) for the stereochemical extremes (structures 1 and 3) is consistent with the observation of intermediate arrangements (structure 2) and their ready interconversion between three different stereochemistries. Dimerization in the case of PhHg(meoxine) has been explained by donation of a pair of electrons from oxygen of one meoxine to an empty *p* orbital of an *sp*-hybridized mercury atom.

(b) In the complex $(C_6F_5)_2Hg(mda)_{1/2}$, the *sp*-hybrid bonding model explains the T-shaped distribution of the two C_6F_5(C–Hg–C, 173°) and one arsenic atom with a Hg–As distance of 3.40 Å (within the sum of van der Waals radii).

(c) A t.g.a. study of complexes of bidentate nitrogen donors with $(C_6F_5)_2Hg$ reveals that all the ligands except bpy behave as bidentates (Table 2) [27,28]. This different behaviour can be explained if $Hg(C_6F_5)_2$ remains linear in the adducts, and the newly formed Hg–N bonds (with phen, en, etc.) involve only *p* orbitals in the plane normal to the C–Hg–C axis. The coordinated phen molecule should be planar and could be expected to give good overlap between the donor orbitals on the nitrogen atoms and these *p* orbitals. A coordinated bipy molecule, however, must be twisted to avoid clashing of the 3,3′-H atoms, and this leads to the donor electrons on the nitrogen atoms being directed well away from the mercury atom, so that only poor overlap can be expected and consequently weak Hg–N bonds result. A similar twist can be expected with coordinated diamines, but in this case due to the sp^3 hybridization of the nitrogen atom orbitals, the donor orbitals still overlap well with the mercury *p* orbitals and strong Hg–N bonds can be expected.

(d) The nature of the bonding in Ph_2HgL_2 (L = phen, L-dmp, etc.) can be readily explained. In the adducts Ph_2HgL_2, the crystal structure shows that there is one ligand per Ph_2Hg moiety and the other ligand is not coordinating (Fig. 2). Since C–Hg–C is linear, the ligand donor can overlap with one *p* orbital of mercury (e.g. p_y or p_z, assuming that the other p_x orbital is used

in *sp* hybridization). This description is based on the same criterion used for one of the stereochemistries of PhHg(oxine) wherein one *sp*-hybrid orbital was shown interacting with the nitrogen and oxygen donor atoms simultaneously.

(e) Further support for the *sp*-hybrid bonding model comes from X-ray structure determinations of $[MeHg(py_2CH_2)](NO_3)$ and $[MeHg(Et_3terpy)](NO_3)$. The first complex, with bidentate py_2CH_2, has a T-shaped structure with nearly linear C–Hg–N (172°), one strong Hg–N bond (2.16 Å) and one weaker Hg–N′ bond (2.75 Å). In the second complex, Et_3terpy is tridentate and there is again a nearly linear C–Hg–N moiety (171°) with a central Hg–N distance of 2.26 Å. The other two terminal nitrogen atoms have longer Hg–N distances (2.51 and 2.61 Å).

The same bonding model may be used to explain the nature of the bonding in other complexes. In brief, the *sp*-hybrid bonding model emerges as the acceptable model to explain the nature of bonding in organomercury(II) complexes. It may be appropriate to add here that the bonding in mercury(II) complexes or analogous systems formally described as sp^2, sp^3, sp^3d^2, etc. may only be an oversimplification of the true bonding situation. The real bonding description requires both X-ray data and theoretical considerations.

E. CONCLUSIONS AND FUTURE SCOPE OF STUDIES

From this survey, a number of important conclusions have been drawn. These are briefly discussed below.

(i) Factors controlling complex formation by organomercury(II)

The ability of two-coordinate mercury to form complexes with bases is very dependent upon the nature of the groups attached to mercury. Thus, while mercury(II) halides are known to form a wide range of adducts with both monodentate and bidentate ligands, no complexes have been isolated with mercury dialkyls. The relative electronegativities of mercury and the adjoining groups, together with the resulting influence upon the formal charge on mercury, appear to play an important role in complex formation. Thus, the inability of mercury(II) dialkyls to form stable complexes may be a reflection of the similar electronegativities of alkyl groups (ca. 2.3) and mercury (1.9), and hence the resulting low formal charge on mercury. The replacement of alkyl by more electronegative groups would be expected to enhance stable complex formation. Certainly, the presence of a halogen in the organomercury halides, RHgX, does appear to increase the acceptor character of mercury. Consequently, a number of complexes have been

reported for a range of R and X. The substitution in R_2Hg by electron-withdrawing substituents in R should also increase the formal charge on mercury, thereby increasing the formation of stable addition compounds. Thus, bis(trinitromethyl)mercury and bis(fluoroalkyl) mercurials form a wide range of isolable complexes, in contrast to the mercury dialkyls themselves. Similarly, where diphenylmercury only gives rise to weak complexes of the type Ph_2HgL_2 (L = phen, etc., a bidentate ligand), bis(pentafluorophenyl) mercury(II) forms numerous stable addition complexes. The lack of complex formation by $(C_6Cl_5)_2Hg$ appears to be due to possible coordination by chlorine atoms in *ortho* positions [80].

(ii) Uniqueness of the sp*-hybrid bonding model*

In Section D, it was amply demonstrated that the nature of bonding in various organomercury(II) complexes can be explained by a single *sp*-hybrid bonding model. Support for this model comes from X-ray diffraction studies giving different bond distances for mercury when the group involved in bonding uses an *sp*-hybrid orbital on mercury or overlaps with a *p* orbital on mercury perpendicular to the C–Hg–Y axis (Y = C, Cl, Br).

(iii) ^{199}Hg NMR as a useful tool for mercury(II) coordination chemistry

As discussed in Section C(iv), ^{199}Hg NMR holds promise for reliable study of the coordination chemistry of mercury(II). It is capable of determining the number of ligands bound to the mercury atom. The only requirement is that the complex be soluble in a suitable solvent. There is also a lack of useful correlations as mentioned earlier. Nevertheless, in view of the limited useful techniques available, ^{199}Hg NMR may become quite popular among chemists in future.

(iv) Factors responsible for the higher stability of the complexes of some mercurials

(a) Chelate effect

In the thermodynamic studies section, it was shown that complexes of bidentate ligands such as phen and en and their derivatives forming five-membered rings are more stable than those forming six or higher membered rings. Furthermore, the monodentate ligands form less stable complexes than bidentates. These observations reveal that the chelate effect is an important factor in forming more stable complexes.

(b) Effect of substituents in ArHgX on adduct stability

In the phen adduct with ArHgX, the adduct stability is raised by chlorine

substitution in the aryl group and lowered by alkyl or alkoxy substitution, notwithstanding the fact that the enthalpy of formation remains nearly the same. This difference is attributed to the higher bond strength of $Hg-C_6Cl_5$ over $Hg-C_6H_5$. The higher bond strength may be due to the effect of the increased polarity of the $Hg-C_6Cl_5$ bond because of the higher electronegativity of the C_6Cl_5 group. However, this should have given a higher value for the enthalpy of formation due to enhanced Lewis acidity of mercury which is not the case observed experimentally. In addition, it appears very probable that lone pairs of electrons on chlorine atoms adjacent to mercury are playing some role in reducing the Lewis acidity of mercury by transferring some charge density from the ring to the mercury atom. This phenomenon would keep the Lewis acidity nearly constant. The alternate interaction involves the lone pair of electrons on the chlorine atoms adjacent to mercury forming weak bonds between mercury(II) and chlorine. Further investigation is needed for substantiating these interaction mechanisms.

The higher stability of the complexes of RHgX when R is an aryl group over those when R is an alkyl group may also be explained in terms of the higher thermodynamic and kinetic stability of the Hg–Ar bond (see also (i) above).

(v) Future scope of studies

It is apparent from this survey that a great deal of work needs to be done using ligands such as phosphines/arsines and their chalcogenides, oxides of bipyridines and phenanthrolines, thioureas, etc. The work on diphenylmercury(II) or diarylmercury(II) bearing different substituents in the aryl group is a challenging field of research activity. Three complexes of Ph_2Hg with phenanthroline ligands are weak complexes and have unusual stoichiometry (1 : 2, metal : ligand). Single crystal X-ray studies must be extended.

ACKNOWLEDGEMENTS

The author thanks the International Union of Crystallography (England); The Royal Society of Chemistry (London); CSIRO Editorial and Publications Service (Australia); Elsevier Sequoia, S.A. Editorial Office (Amsterdam); The American Chemical Society (Washington); and authors for granting permission to reproduce various figures.

REFERENCES

1 D.L. Rabenstein, Acc. Chem. Res., 11 (1978) 100.
2 S. Suzuki, T. Karazava, Y. Hayakawa and K. Tamogami, Chem. Abstr., 57 (1962) 9881f.

3 M. Hannan, H.G. Dickensen and P.P. Hof, Br. Pat. 736,399, Chem. Abstr., 50 (1956) 7877f; Ger. Pat. 943,730, Chem. Abstr., 52 (1958) 11963e.
4 R.O. Weiss and S.J. Lederer, U.S. Pat. 2,844,508, Chem. Abstr., 52 (1958) 19001c; U.S. Pat. 3,130,123, Chem. Abstr., 61 (1964) 3147g; Br. Pat. 841,948; Chem. Abstr., 55 (1961) 2004.
5 J.E.Eg. Matchacek, Plant Dis. Rep., 42 (1958) 529; Chem. Abstr., 52 (1958) 14062h; W.J. Byford, Ann. Appl. Biol., 51 (1963) 41; Chem. Abstr., 60 (1964) 2270b; L.H. Purdy, Plant Dis. Rep., 41 (1957) 976; Chem. Abstr., 52 (1958) 13171g.
6 Y. Takeda, T. Kunugi, O. Hishino and T. Ukita, Toxicol. Appl. Pharmacol., 13 (1968) 156.
7 Y. Takeda, J. Hyg. Chem., 14 (1968) 177.
8 J. Ans, H. Zimmer and H. Bergmann, Chem. Ber., 85 (1952) 583; Chem. Abstr., 46 (1952) 11134i.
9 H. Gilman and R.C. Brown, J. Am. Chem. Soc., 52 (1930) 3314.
10 D. Spinelli and A. Salvemini, Ann. Chim., 50 (1960) 1423; Chem. Abstr., 55 (1961) 10360.
11 T. Eskin, Chem. Abstr., 39 (1945) 1636.
12 M.C. Esquivel, A.S. Macias and L.B. Reventos, J. Inorg. Nucl. Chem., 39 (1977) 1153.
13 G.A. Razuvaev and M.A. Shubenko, Zh. Obshch. Khim., 20 (1950) 175; Chem. Abstr., 44 (1950) 5832h.
14 D. Seyferth and J.M. Burtlitch, J. Organomet. Chem., 4 (1965) 127.
15 J.G. Livingstone, R.D. Chambers, G.E. Coates and W.K.R. Musgrave, J. Chem. Soc. (1962) 4367.
16 H.B. Powell, M.T. Maung and J.J. Lagowskii, J. Chem. Soc. (1963) 2484.
17 A.G. Davies, G.B. Deacon, J.E. Connett and J.H.S. Green, J. Chem. Soc. (C), (1966) 106.
18 G.B. Deacon, C.G. Barraclough and G.E. Berkovic, Aust. J. Chem., 30 (1977) 1905.
19 J.H.S. Green, Spectrochim. Acta, Part A, 24 (1968) 863.
20 A.J. Canty and G.B. Deacon, Inorg. Nucl. Chem. Lett., 5 (1969) 183.
21 A.J. Canty and G.B. Deacon, J. Organomet. Chem., 49 (1973) 125.
22 A.J. Canty and B.M. Gatehouse, Acta Crystallogr., Sect. B, 28 (1972) 1872.
23 M. Cano, A. Santos and L. Ballester, An. Quim., 73 (1977) 1051; Chem. Abstr., 88 (1978) 105503m.
24 L.I. Zakharkin and L.S. Podvisotskaya, Zh. Obshch. Khim., 39 (1969) 929.
25 A.J. Canty and G.B. Deacon, Aust. J. Chem., 24 (1971) 489.
26 A.J. Canty and B.M. Gatehouse, J. Chem. Soc., Dalton Trans., (1972) 511.
27 Y. Farhangi and D.P. Graddon, J. Organomet. Chem., 71 (1974) 17.
28 W.H. Puhl and H.F. Henneike, J. Phys. Chem., 77 (1973) 558.
29 G.B. Deacon and J.E. Connett, J. Chem. Soc. (C), (1966) 1058.
30 J.J. Lagowski and H.B. Powell, J. Chem. Soc. (A), (1966) 1282.
31 Z.A. Stumbrevichyute, L.A. Fedorov, B.L. Dyatkin and B.I. Martynov, Russ. J. Org. Chem., (1975) 2033.
32 N.A. Bell, I.W. Nowell, P.A. Reynolds and R.J. Lynch, J. Organomet. Chem., 193(2) (1980) 147.
33 J.H.S. Green, Spectrochim. Acta, Part A, 24 (1968) 863.
34 J.D. Miller and W.R. McWhinnie, Adv. Inorg. Chem. Radiochem., 12 (1969) 135.
35 E.G. Puebla, A. Vegas, S. Garcia-Blanco, Acta Crystallogr., Sect. B, 34(11) (1978) 3382.
36 A.J. Canty and A. Marker, Inorg. Chem., 15 (1976) 425.
37 A.J. Canty, A. Marker and B.M. Gatehouse, J. Organomet. Chem., 88 (1975) C31.
38 A.J. Canty, N. Chaichit and B.M. Gatehouse, Acta Crystallogr., Sect. B, 34 (1978) 3229.

39 A. Ruiz-Amil, S. Martinez-Carrera and S. Garcia-Blanco, Acta Crystallogr., Sect. B, 34 (1978) 2711.
40 H.B. Buergi, E. Fischer, R.W. Kunz, M. Parvez and P.S. Pregosin, Inorg. Chem., 21 (1982) 1246.
41 R.L. Raston, B.W. Skelton and A.H. White, Aust. J. Chem., 31 (1978) 537.
42 A.J. Canty, N. Chaichit, B.M. Gatehouse, E.E. George and G. Hayhurst, Inorg. Chem., 20 (1981) 2414.
42 (a) F.A.L. Anet and J.L. Sudmeier, J. Magn. Reson., 1 (1969) 124; (b) H.F. Henneike, J. Am. Chem. Soc., 94 (1972) 5945.
43 D. Grdenic, Q. Rev. Chem. Soc., 19 (1965) 303.
44 L.H. Jones, Inorganic Vibration Spectroscopy, Vol. 1. Marcel Dekker, New York, 1971, p. 120.
45 J. Mink, G. Vegh and Y.A. Pentin, J. Organomet. Chem., 35 (1972) 225.
46 A.A. Schilt and R.C. Taylor, J. Inorg. Nucl. Chem., 9 (1959) 211.
47 F.A. Cotton, R.D. Barnes and E. Bannister, J. Chem. Soc., (1960) 2199.
48 J.C. Sheldon and S.Y. Tyree, J. Am. Chem. Soc., 80 (1958) 4775.
49 D.M.L. Goodgame and F.A. Cotton, J. Chem. Soc., (1961) 2298.
50 J.H.S. Green and G.B. Deacon, Chem. Ind., (1965) 1031.
51 J.H.S. Green and G.B. Deacon, Spectrochim. Acta, Part A, 24 (1968) 845.
52 R.J.H. Clark, Spectrochim. Acta, 21 (1965) 955.
53 E. König, K. Madeja and K.J. Watson, J. Am. Chem. Soc., 90 (1968) 1146.
54 R.G. Inskeep, J. Inorg. Nucl. Chem., 24 (1962) 763.
55 R.J.H. Clark and C.S. Williams, Spectrochim. Acta, 21 (1965) 1861.
56 C. Postmus, J.R. Ferraro and W. Wozmak, Inorg. Chem., 6 (1967) 2030.
57 F. Farha and R.T. Iwamoto, Inorg. Chem., 4 (1965) 844.
58 M. Halman and S. Pinchas, J. Chem. Soc., (1958) 3264.
59 D.R. Marks, D.J. Phillips and J.P. Redfern, J. Chem. Soc. (A), (1967) 1464.
60 A. Sabatini and S. Califano, Spectrochim. Acta, 16 (1960) 677.
61 (a) V.S. Petrosyan and O.A. Reutov, Pure appl. Chem., 37 (1974) 147; (b) J. Relf, R.P. Cooney and H.F. Hennike, J. Organomet. Chem., 39 (1972) 75.
62 J.N. Baxter, J.C. Craig and J.B. Willis, J. Chem. Soc., (1955) 669.
63 F.A. Cotton, in J. Lewis and R.G. Wilkins (Eds.), Modern Coordination Chemistry, Interscience, New York, 1967, 363 pp.
64 H.B. Powell and J.J. Lagowskii, J. Chem. Soc. (A), (1966) 1282.
65 L. Pauling, The Nature of the Chemical Bond, 3rd edn. Cornell University Press, Ithaca, New York.
66 G. Dwyer, D.C. Goodall, R.H.B. Mais, H.M. Powell and L.M. Venanzi, J. Chem. Soc. (A), (1966) 1110.
67 A.T. McPhail and G.A. Sim, Chem. Commun., (1966) 121.
68 S. Kulpa, Z. Anorg. Chem., 349 (1967) 314.
69 W.R. Cullen, Can. J. Chem., 38 (1960) 439.
70 W.R. Cullen, Can. J. Chem., 39 (1961) 2486.
71 E. Pitcher and F.G.A. Stone, Spectrochim. Acta, 18 (1962) 585.
72 A.J. Downs, J. Chem. Soc., (1963) 5273.
73 T.N. Bell, B.J. Pullman and B.O. West, Aust. J. Chem., 16 (1963) 636.
74 G.K. Semin, T.A. Babushkina and G.G. Yakobson, Nuclear Quadrupole Resonance in Chemistry. Wiley, New York, 1975.
75 C.H. Townes and B.P. Dailey, J. Chem. Phys., 17 (1949) 1782.
76 D. Seyferth and R.H. Towe, Inorg. Chem., 1 (1962) 185.

77 A.J. Canty, G.B. Deacon and P.W. Felder, Aust. J. Chem., 21 (1968) 1757.
78 G.B. Deacon, R.J. Bertino and J.M. Miller, Aust. J. Chem., 31 (1978) 527.
79 A.J. Canty, G.B. Deacon and P.W. Felder, Inorg. Nucl. Chem. Lett., 3 (1967) 263.
80 G.B. Deacon and P.W. Felder, Aust. J. Chem., 19 (1966) 2381.
81 A.J. Canty and G.B. Deacon, Inorg. Nucl. Chem. Lett., 4 (1968) 125.
82 H. Tanaka, Y. Hojo and Y. Sugiura, J. Inorg. Nucl. Chem., 39 (1977) 715.
83 G.E. Coates and A. Lauder, J. Chem. Soc., (1965) 1857.
84 R.J. Cross, A. Lauder and G.E. Coates, Chem. Ind., (1962) 2013.
85 R.E. Dessy, W.L. Budde and C. Woodruff, J. Am. Chem. Soc., 84 (1962) 1172.
86 N.A. Bell, I.W. Nowell and D.J. Starkey, Inorg. Chim. Acta, 48(2) (1981) 139.
87 C.C. Addison, N. Logan, S.C. Wallwork and C.D. Garner, Chem. Soc. Rev., 25 (1971) 289.
88 A.J. Canty, A. Marker, P. Barron and P.C. Healy, J. Organomet. Chem., 144 (1978) 371.
89 A.J. Canty and B.M. Gatehouse, J. Chem. Soc., Dalton Trans., (1976) 2018.
90 A.J. Canty, G. Hayhurst, N. Chaichit and B.M. Gatehouse, J. Chem. Soc., Chem. Commun., (1980) 316.
91 R.J.P. William and L. Morpurgo, J. Chem. Soc. (A), (1966) 73.
92 (a) G. Faraglia, L. Ronucci and R. Barbieri, Gazz. Chim. Ital., 93 (1963) 1413. (b) R. Barbieri, G. Giustiniani and L. Ronucci, J. Inorg. Nucl. Chem., 26 (1964) 203.
93 (a) T. Moeller and A.J. Cohen, J. Am. Chem. Soc., 72 (1950) 3546. (b) T. Moeller and F.L. Pundsack, J. Am. Chem. Soc., 76 (1954) 617.
94 M. Wada and R. Okawara, Inorg. Nucl. Chem. Lett., 5 (1969) 355.
95 K. Sone, J. Am. Chem. Soc., 75 (1953) 5207.
96 L. Roncucci, G. Faraglia and R. Barbieri, J. Organomet. Chem., 6 (1966) 2781.
97 H.A. Meinema, E. Rivarola and J.G. Noltes, J. Organomet. Chem., 17 (1969) 71.
98 M. Wada, T. Suda and R. Okawara, J. Organomet. Chem., 65 (1974) 335.
99 M. Aritomi and Y. Kawasaki, J. Organomet. Chem., 81 (1974) 363.
100 R.D. Chambers and T. Chivers, Organomet. Chem. Rev., 1 (1966) 279.
101 U.S. Nandi, J.C. Wang and N. Davidson, Biochemistry, 4 (1965) 1687.
102 D.C. Craig, Y. Farahangi, D.P. Graddon and N.C. Stephenson, Cryst. Struct. Commun., 3 (1973) 154.
103 A.L. Beauchamp, B. Saperas and R. Rivest, Can. J. Chem., 52 (1974) 2923.
104 I.P. Beletskaya, K.P. Butin, A.N. Ryabtsev and O.A. Reutov, J. Organomet. Chem., 59 (1973) 1.
105 S.C. Jain and R. Rivest, Inorg. Chim. Acta, 4 (1970) 291.
106 M. Esquivel, A. Macias and L.B. Reventos, An. Quim., 71 (1975) 831; Chem. Abstr., 84 (1976) 173131f.
107 I.S. Ahuja and Raghubir Singh, J. Coord. Chem., 4 (1975) 181.
108 R.M. Izatt, D. Eatough and J.J. Christensen, J. Phys. Chem., 72 (1963) 2720.
109 R.J. Izatt, C.H. Bartholomew, C.E. Morgan, D.J. Eatough and J.J. Christensen, Thermochim. Acta, 2 (1971) 313.
110 E.C. Porzsolt, M.T. Beck and A. Bitto, Chem. Abstr., 81 (1974) 69184c.
111 I.S. Ahuja, R. Sriramulu and R. Singh, Indian J. Chem., 18A(2) (1979) 188.
112 H. Schmidbauer and K.H. Raethlein, Chem. Ber., 106 (1973) 2491.
113 E.C. Porzsolt, B. Mohai and M.T. Beck, Chem. Abstr., 81 (1974) 85408j.
114 R.G. Goel, W.P. Henry and W.O. Ogini, Can. J. Chem., 57(7) (1979) 762.
115 S.C. Jain, J. Inorg. Nucl. Chem., 35 (1973) 413.
116 A.L. Fridman, T.N. Ivshina, V.P. Ivshin, V.A. Tartakovskii and S.S. Novikov, Izv. Akad. Nauk SSSR, Ser. Khim., (1971) 2279; Chem. Abstr., 76 (1972) 99787r.

117 R. Colton and D. Dakternicks, Aust. J. Chem., 34(2) (1981) 323.
118 L.H. Jones, Inorg. Chem., 13 (1974) 2289.
119 D.A. Dows, A. Haim and W.K. Wilmarth, J. Inorg. Nucl. Chem., 21 (1961) 33.
120 R.A. Decastello, C.P. MacCall, N.B. Egen and A. Haim, Inorg. Chem., 8 (1969) 699.
121 S.O. Grim and D.P. Shah, Inorg. Nucl. Chem. Lett., 14 (1978) 105.
122 T. Allman, R.G. Goel and P. Pilon, Can. J. Chem., 57 (1979) 91.
123 L.A. Fedorov, E.I. Fedin, B.A. Kvasov and I.P. Beletskaya, Zh. Strukt. Khim., 10 (1969) 247; J. Struct. Chem., 10 (1969) 231.
123 (a) G.E. Maciel and M. Borzo, J. Magn. Reson., 10 (1973) 388. (b) G.P. Maciel and M. Borzo, J. Magn. Reson., 19 (1975) 279. (c) M.A. Sens, N.K. Wilson, P.D. Ellis and J.D. Odom, J. Magn. Reson., 19 (1975) 323.
124 J.A. Hatton, W.G. Schneider and W. Siebrand, J. Chem. Phys., 39 (1963) 1330.
125 H.F. Henneike, J. Am. Chem. Soc., 94 (1972) 5945.
126 E.F. Kiefer, W.L. Waters and D.A. Carlson, J. Am. Chem. Soc., 90 (1968) 5127.
127 R. Colton and D. Dakternieks, Aust. J. Chem., 33 (1980) 955.
128 E.C. Alyea, G. Ferguson and R.J. Restivo, J. Chem. Soc., Dalton Trans., (1977) 1845.
129 F.G. Moers and J.P. Laughout, Recl. Trav. Chim. Pays-Bas, 92 (1973) 996.
130 S.O. Grim, P.J. Lui and R.L. Keiter, Inorg. Chem., 13 (1974) 342.
131 T. Allman and R.G. Goel, Inorg. Nucl. Chem. Lett., 15 (1979) 199.
132 D.P. Graddon and J. Mondal, J. Organomet. Chem., 107 (1976) 1.
133 D.P. Graddon and R.K. Nanda, J. Organomet. Chem., 132 (1977) 1.
134 A.C. Dash and R.K. Nanda, J. Indian Chem. Soc., 50 (1973) 808.
135 D.P. Graddon and J. Mondal, J. Organomet. Chem., 159 (1978) 9.
136 D.P. Graddon and Y. Farhangi, Aust. J. Chem., 27 (1974) 2103.